



The Burgers Program for Fluid Dynamics

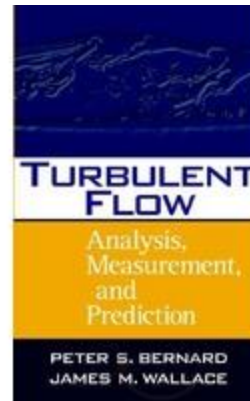


Tutorial School on Fluid Dynamics: Aspects of Turbulence

Session I: Refresher Material

Instructor: James Wallace

Adapted from



*Publisher: John S. Wiley & Sons
2002*



*Center for Scientific Computation
and Applied Mathematical Modeling*



*Institute for Physical Science
and Technology*

Center for Environmental
& Applied Fluid Mechanics

Johns Hopkins University



National Science Foundation

Transport equations

Describe how properties of a fluid element change, as given by the substantial derivative, $D(\)/Dt$, as the element is transported through the flow field.

Mass conservation

$$\frac{\partial U_i}{\partial x_i} = 0, \quad U_i = \bar{U}_i + u_i,$$

$$\frac{\partial}{\partial x_i} \overline{(\bar{U}_i + u_i)} = 0.$$

$$\frac{\partial \bar{U}_i}{\partial x_i} = 0$$

$$\frac{\partial u_i}{\partial x_i} = 0$$

mean and fluctuating velocity components are divergence free

Momentum conservation

Navier-Stokes equation for an incompressible flow (N-S)

$$\rho \frac{\partial U_i}{\partial t} + \rho \frac{\partial}{\partial x_k} (U_k U_i) = -\frac{\partial P}{\partial x_i} + \mu \nabla^2 U_i$$

Decomposing into mean and fluctuating parts, invoking continuity and averaging using Reynolds rules yields

$$\rho \left[\frac{\partial \bar{U}_i}{\partial t} + \frac{\partial}{\partial x_k} (\bar{U}_k \bar{U}_i) \right] = -\frac{\partial \bar{P}}{\partial x_i} + \frac{\partial}{\partial x_k} \left(\mu \frac{\partial \bar{U}_i}{\partial x_k} - \rho \overline{u_i u_k} \right)$$

Reynolds stress tensor

This equation and $\frac{\partial \bar{U}_i}{\partial x_i} = 0$ together are called the Reynolds Averaged Navier-Stokes Equations (RANS). This equation describes the transport of the Mean momentum in the x_i direction

There are more unknowns than the four available equations. To “close” the set of equations the Reynolds stress term must be related to the velocity gradient in some way through a model equation.

Reynolds Shear stress or velocity fluctuation covariance

$$R_{ij} \equiv \overline{u_i u_j}$$

For $i = j$, and summing over i , half this covariance becomes the turbulent kinetic energy (TKE) when multiplied by the density

$$K \equiv \overline{\rho u_i^2} / 2.$$

T

The components of the TKE are related to the variances of the velocity fluctuations

$$\overline{u_1^2}, \overline{u_2^2}, \overline{u_3^2}.$$

The square roots of these variance are the root-mean-square values of the velocity fluctuation components. They are a measure of the amplitudes of the fluctuations.

Reynolds stress transport

By decomposing the N-S equation for momentum and subtracting the RANS equation from it, a transport equation for the momentum of the fluctuations is obtained

$$\rho \left[\frac{\partial u_i}{\partial t} + \frac{\partial}{\partial x_k} (\bar{U}_k u_i) \right] = -\rho u_k \frac{\partial \bar{U}_i}{\partial x_k} - \frac{\partial p}{\partial x_i} + \mu \nabla^2 u_i - \frac{\partial}{\partial x_k} (\rho u_i u_k - \rho \overline{u_i u_k})$$

Multiply the transport equation for the fluctuating momentum, term by term, by The fluctuating velocity components, u_j .

$$\begin{aligned} \rho u_j \left[\frac{\partial u_i}{\partial t} + \frac{\partial}{\partial x_k} (\bar{U}_k u_i) \right] &= -\rho u_j u_k \frac{\partial \bar{U}_i}{\partial x_k} - u_j \frac{\partial p}{\partial x_i} \\ &+ \mu u_j \nabla^2 u_i - u_j \frac{\partial}{\partial x_k} (\rho u_i u_k - \rho \overline{u_i u_k}) \end{aligned}$$

Exchange the subscripts, i and j

$$\begin{aligned} \rho u_i \left[\frac{\partial u_j}{\partial t} + \frac{\partial}{\partial x_k} (\bar{U}_k u_j) \right] &= -\rho u_i u_k \frac{\partial \bar{U}_j}{\partial x_k} - u_i \frac{\partial p}{\partial x_j} \\ &+ \mu u_i \nabla^2 u_j - u_i \frac{\partial}{\partial x_k} (\rho u_j u_k - \rho \overline{u_j u_k}) \end{aligned}$$

Add these last two equations together, average the result and simplify using Reynolds rules to obtain the transport equation for the Reynolds stress tensor.

$$\begin{aligned}
 \frac{\partial}{\partial t} (\rho \overline{u_i u_j}) + \underbrace{\frac{\partial}{\partial x_k} (\overline{U_k \rho u_i u_j})}_{\text{Advection}} = & \underbrace{- \left(\rho \overline{u_i u_k} \frac{\partial \overline{U_j}}{\partial x_k} + \rho \overline{u_j u_k} \frac{\partial \overline{U_i}}{\partial x_k} \right)}_{\text{Production}} \\
 & - \underbrace{\frac{\partial}{\partial x_k} (\rho \overline{u_i u_j u_k})}_{\text{Turbulent diffusion}} \\
 & \underbrace{\frac{\partial}{\partial x_k} (\overline{p u_i} \delta_{jk} + \overline{p u_j} \delta_{ik})}_{\text{Pressure diffusion}} + \underbrace{2 \overline{p s_{ij}}}_{\text{Pressure-strain}} \\
 & + \underbrace{\mu (\overline{u_i \nabla^2 u_j} + \overline{u_j \nabla^2 u_i})}_{\text{Viscous diffusion \& Dissipation}} .
 \end{aligned}$$

Turbulent kinetic energy conservation

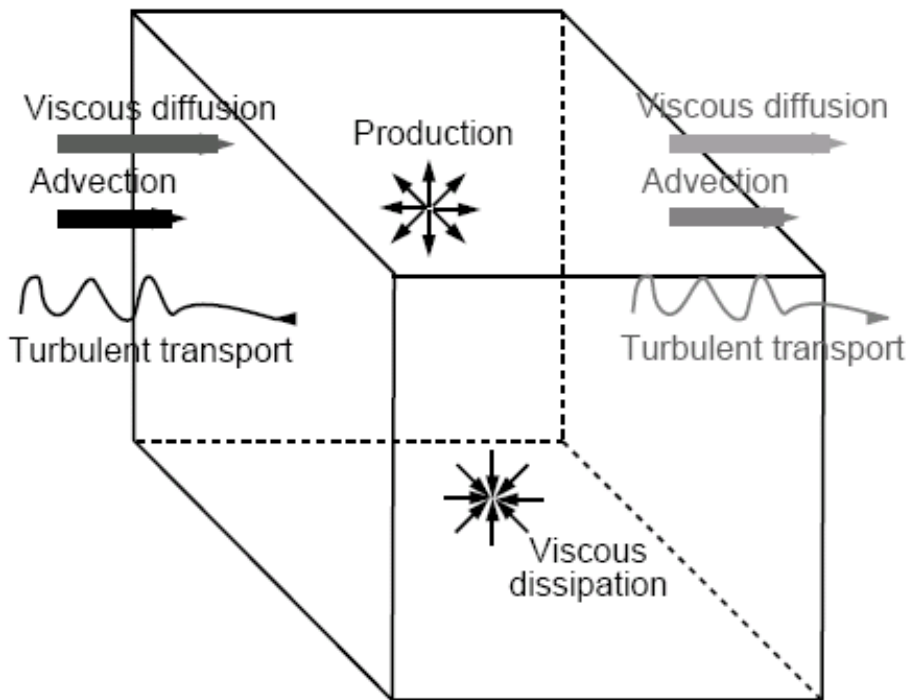
Let $i = j$ in the turbulent transport equation and divide each term by 2ρ to obtain the transport equation for turbulent kinetic energy (per unit mass).

Here \mathcal{K} is $u_i u_i / 2$.

$$\frac{\partial \mathcal{K}}{\partial t} + \underbrace{\frac{\partial}{\partial x_k} (\bar{U}_k \mathcal{K})}_{\text{Advection}} = \underbrace{-\bar{u}_i \bar{u}_k \frac{\partial \bar{U}_i}{\partial x_k}}_{\text{Production}} - \underbrace{\frac{\partial}{\partial x_k} \left(\frac{1}{2} \overline{u_i u_i u_k} \right)}_{\text{Turbulent diffusion}} - \underbrace{\frac{\partial}{\partial x_k} \left(\frac{\overline{p u_k}}{\rho} \right)}_{\text{Pressure diffusion}} + \underbrace{\overline{\nu u_i \nabla^2 u_i}}_{\text{Viscous diffusion \& Dissipation}} \quad \text{(turbulent transport)}$$

Transport in Sources and sinks Transport out

$$\overline{\nu u_i \nabla^2 u_i} = \nu \nabla^2 \mathcal{K} - \nu \frac{\partial u_i}{\partial x_k} \frac{\partial u_i}{\partial x_k}$$



full dissipation rate

$$\nu \frac{\partial u_i}{\partial x_k} \left(\frac{\partial u_i}{\partial x_k} + \frac{\partial u_k}{\partial x_i} \right) = 2\nu \overline{s_{ij} s_{ij}}$$

Only for isotropic turbulence where

$$\begin{aligned} \nu \frac{\partial^2}{\partial x_i \partial x_k} (\overline{u_i u_k}) &= \nu \frac{\partial u_i}{\partial x_k} \frac{\partial u_k}{\partial x_i} \\ &= 0 \end{aligned}$$

does it represent the full dissipation rate.

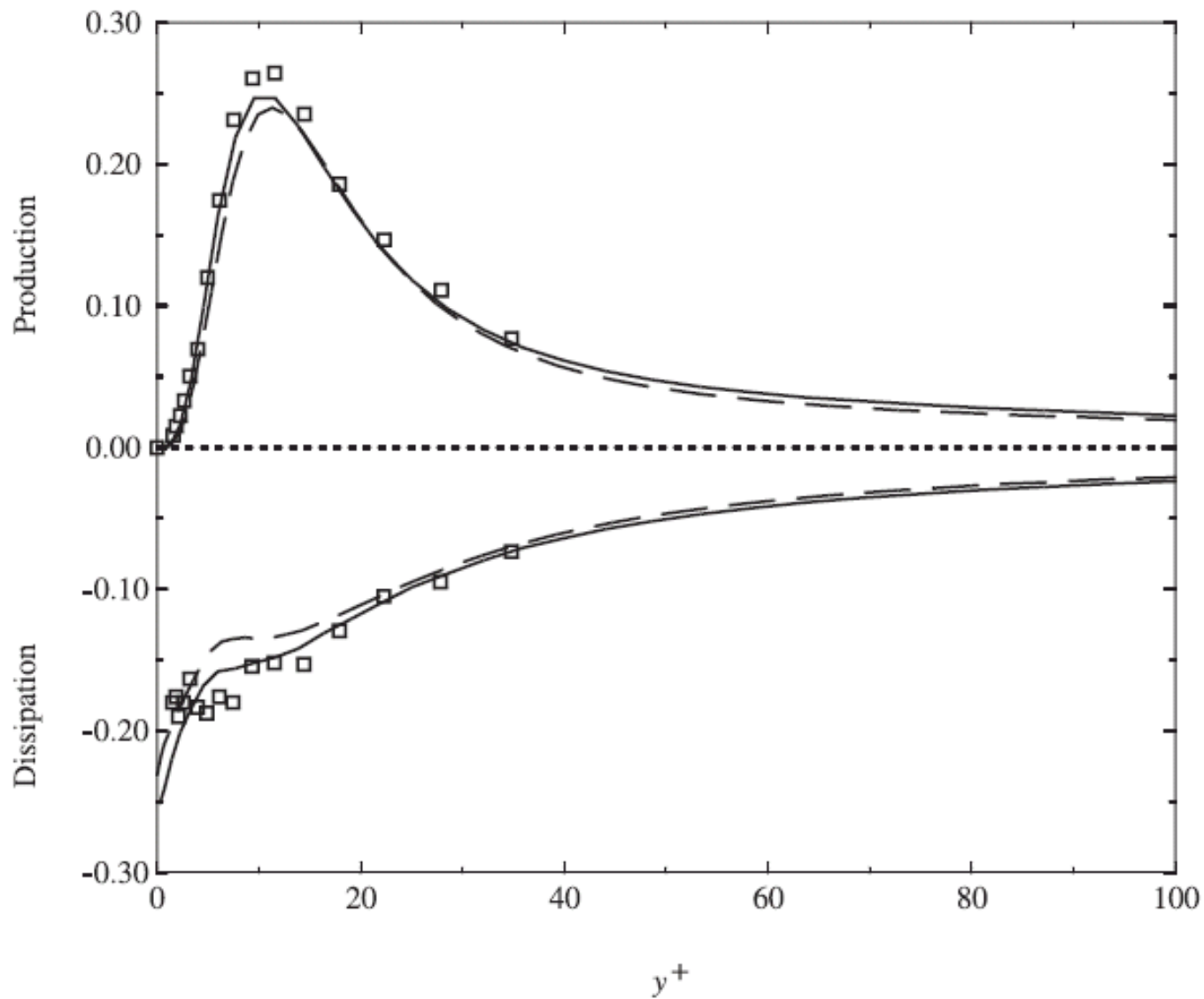


Fig. 4.11 Comparison of turbulent boundary layer and channel flow production and dissipation rates scaled with ν and u_τ . \square , boundary layer measurements at $R_\tau = 1050$ [33]; —, DNS boundary layer at $R_\tau = 650$ [60]; --, DNS channel flow $R_\tau = 590$ [49].

$$\begin{aligned} \overline{\varepsilon}/\nu = & 2\overline{\left(\frac{\partial u}{\partial x}\right)^2}_I + \overline{\left(\frac{\partial u}{\partial y}\right)^2}_{II} + \overline{\left(\frac{\partial u}{\partial z}\right)^2}_{III} + \overline{\left(\frac{\partial v}{\partial x}\right)^2}_{IV} \\ & + 2\overline{\left(\frac{\partial v}{\partial y}\right)^2}_V + \overline{\left(\frac{\partial v}{\partial z}\right)^2}_{VI} + \overline{\left(\frac{\partial w}{\partial x}\right)^2}_{VII} + \overline{\left(\frac{\partial w}{\partial y}\right)^2}_{VIII} \\ & + 2\overline{\left(\frac{\partial w}{\partial z}\right)^2}_{IX} + 2\overline{\left(\frac{\partial u}{\partial y}\right)\left(\frac{\partial v}{\partial x}\right)}_X + 2\overline{\left(\frac{\partial u}{\partial z}\right)\left(\frac{\partial w}{\partial x}\right)}_{XI} \\ & + 2\overline{\left(\frac{\partial v}{\partial z}\right)\left(\frac{\partial w}{\partial y}\right)}_{XII} \end{aligned}$$

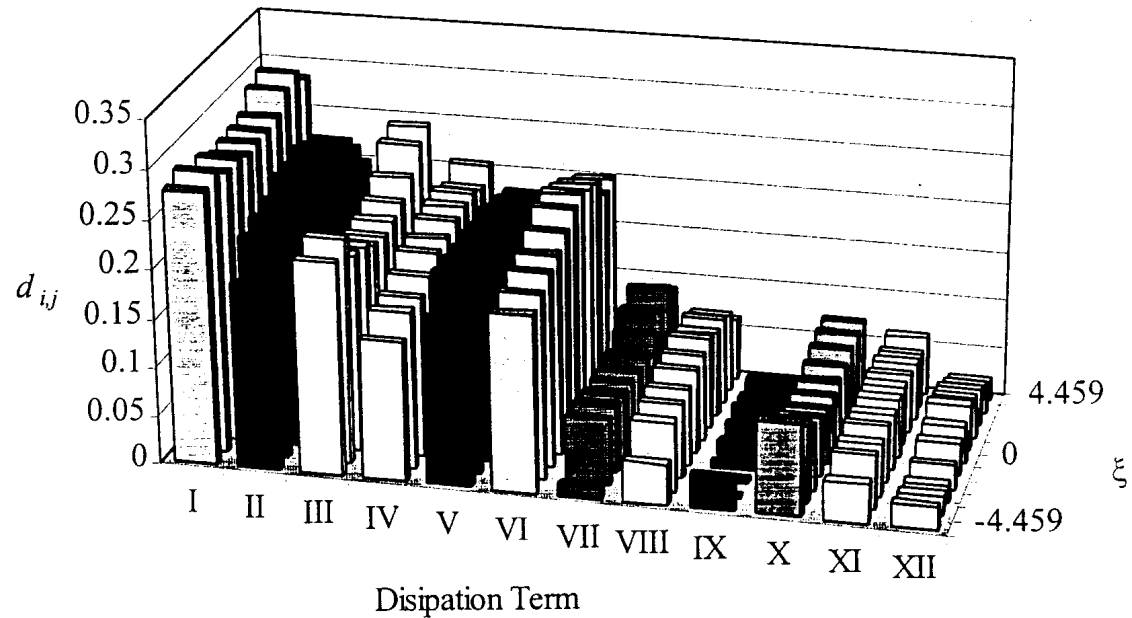


Figure 5.54 Average fractional contribution of each dissipation rate term for each measurement location across the mixing layer, $Re_\theta = 1792$

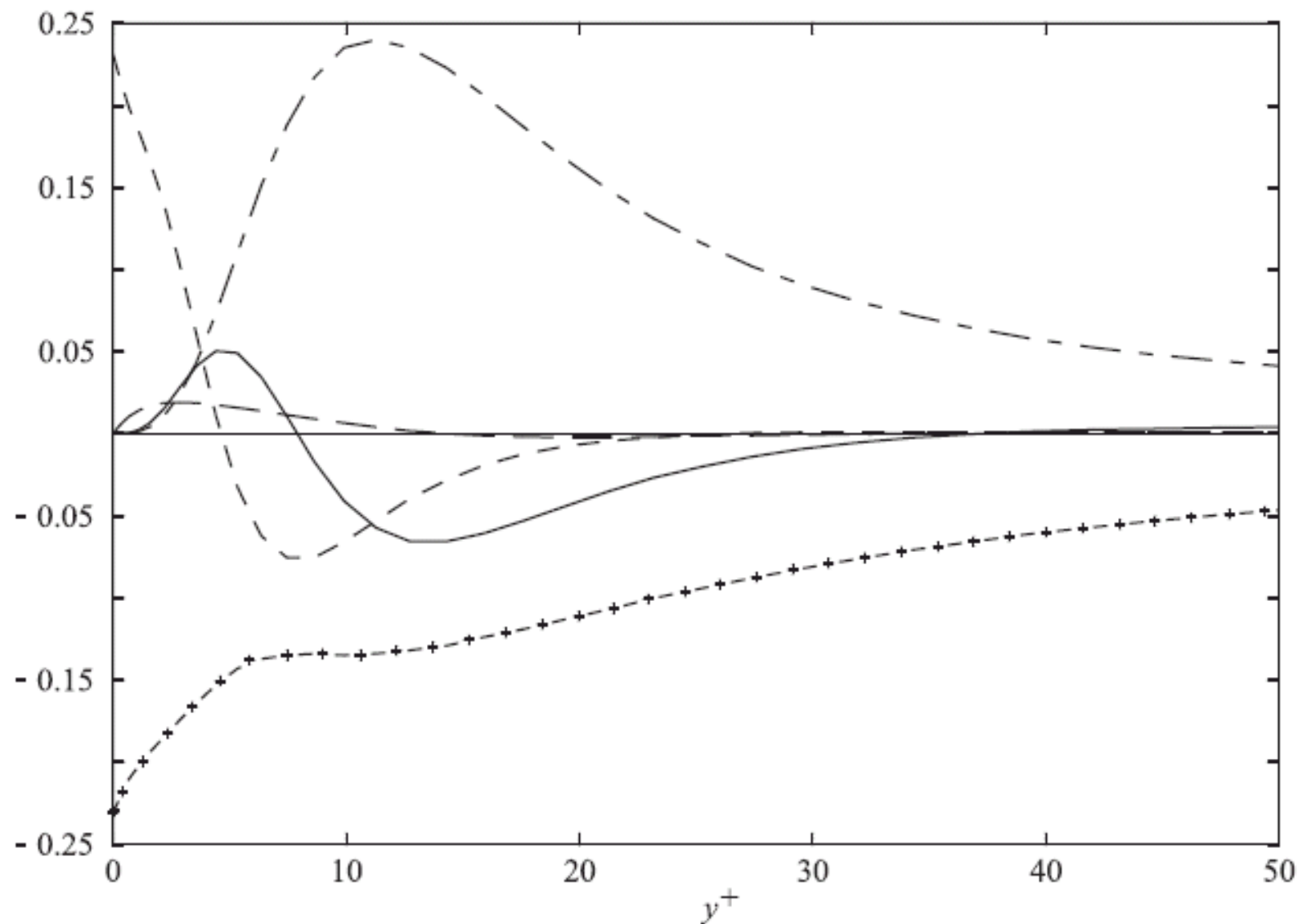


Fig. 4.10 Turbulent kinetic energy budget in channel flow $R_\tau = 590$ scaled with ν and u_τ . — — —, production; — + —, dissipation; — —, pressure work; — —, viscous diffusion; —, turbulent transport. (From [49].)

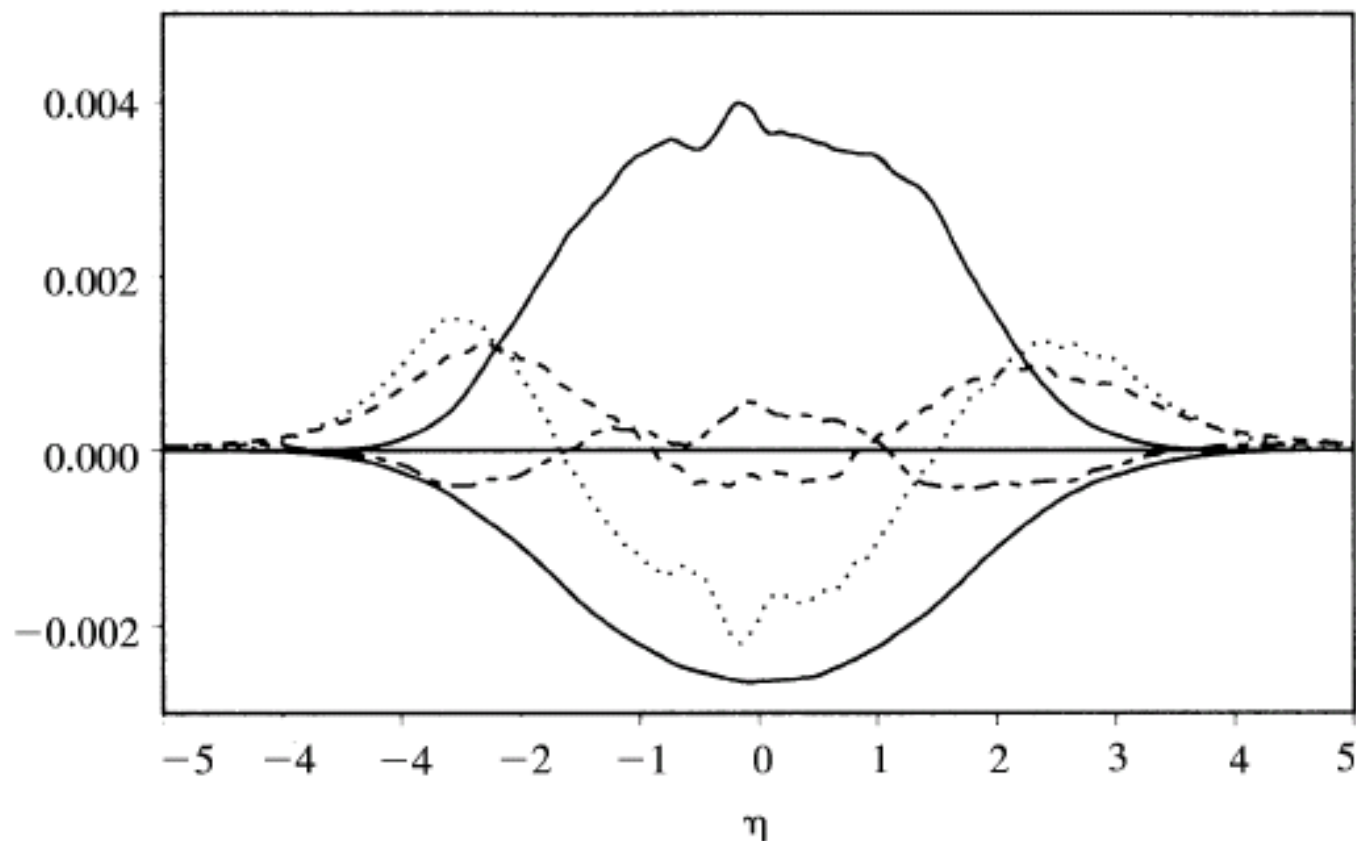


Fig. 5.23 Turbulent kinetic energy balance in two-stream mixing layer for $R_\theta = 1500 - 2000$. —, production (positive curve) and dissipation rate (negative curve); - -, time derivative; ···, turbulent diffusion — · —, pressure diffusion. Terms made nondimensional by ΔU^3 and θ . (From [32].)

Vorticity and enstrophy transport

vorticity Ω_i is defined as the curl of the velocity:

$$\Omega_i = \epsilon_{ijk} \frac{\partial U_k}{\partial x_j}.$$

by taking the curl of the Navier-Stokes equations (3.6) in vorticity form:

$$\epsilon_{pqi} \frac{\partial}{\partial x_q} \left[\frac{\partial U_i}{\partial t} + \frac{\partial}{\partial x_i} \left(\frac{U_k U_k}{2} \right) - \epsilon_{ijk} U_j \Omega_k \right] = \epsilon_{pqi} \frac{\partial}{\partial x_q} \left[-\frac{1}{\rho} \frac{\partial P}{\partial x_i} + \nu \nabla^2 U_i \right]$$

The Instantaneous Vorticity Transport Equation is obtained

$$\frac{\partial \Omega_i}{\partial t} + \frac{\partial}{\partial x_j} (U_j \Omega_i) = \Omega_j \frac{\partial U_i}{\partial x_j} + \nu \nabla^2 \Omega_i.$$

Averaged Vorticity Transport Equation

$$\frac{\partial \bar{\Omega}_i}{\partial t} + \bar{U}_j \frac{\partial \bar{\Omega}_i}{\partial x_j} = \bar{\Omega}_j \frac{\partial \bar{U}_i}{\partial x_j} + \overline{\omega_j \frac{\partial u_i}{\partial x_j}} + \frac{\partial}{\partial x_j} \left(\nu \frac{\partial \bar{\Omega}_i}{\partial x_j} - \overline{u_j \omega_i} \right)$$

Multiply the instantaneous vorticity transport equation term by term with $\Omega / 2$, average and separate the last term into its diffusive and dissipative parts to obtain an averaged transport equation for enstrophy, $\overline{\Omega_i \Omega_i} / 2$

$$\begin{aligned}
 \frac{\partial}{\partial t} \frac{\overline{\Omega_i \Omega_i}}{2} + \underbrace{\frac{\partial}{\partial x_j} \left(U_j \frac{\overline{\Omega_i \Omega_i}}{2} \right)}_{\text{Advection}} &= \underbrace{\overline{\Omega_i \Omega_j \frac{\partial U_i}{\partial x_j}}}_{\text{Rotation and stretching}} \\
 + \underbrace{\nu \nabla^2 \frac{\overline{\Omega_i \Omega_i}}{2}}_{\text{Viscous diffusion}} - \underbrace{\nu \left(\frac{\partial \overline{\Omega_i}}{\partial x_j} \frac{\partial \overline{\Omega_i}}{\partial x_j} \right)}_{\text{Viscous dissipation}}, &
 \end{aligned}$$

This is different from and simpler than the transport equation for mean enstrophy

$$\frac{\overline{\Omega_i \Omega_i}}{2}$$

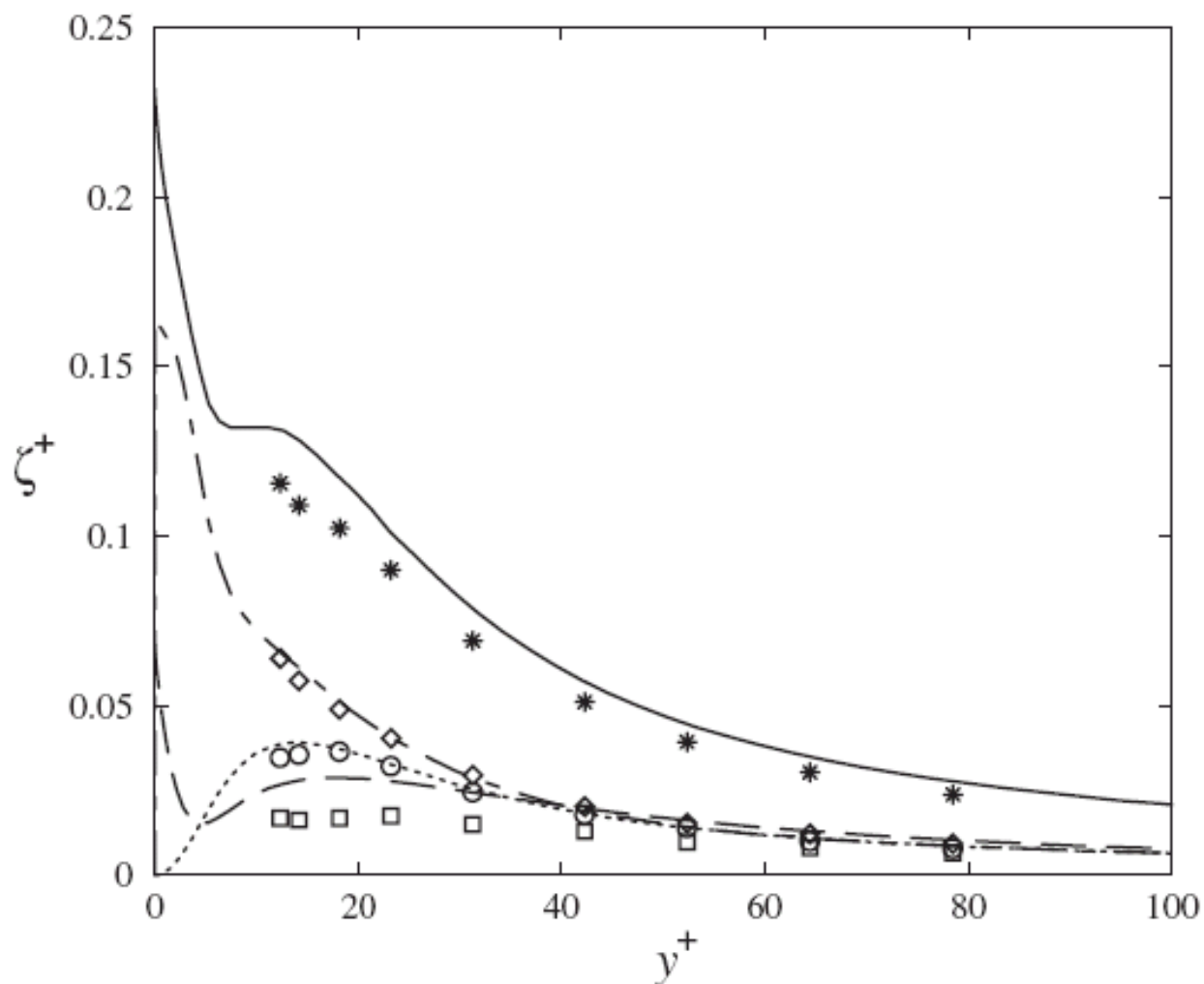


Fig. 4.16 Comparison of enstrophy and its components in channel flow at $R_\tau = 590$ [49] and in a boundary layer at $R_\tau = 1135$ [52]. — — and \square , $\overline{\omega_1^2}^+$; \cdots and \circ , $\overline{\omega_2^2}^+$; — · — and \diamond , $\overline{\omega_3^2}^+$; — and $$, $\zeta^+ = \overline{\omega_1^2}^+ + \overline{\omega_2^2}^+ + \overline{\omega_3^2}^+$.*

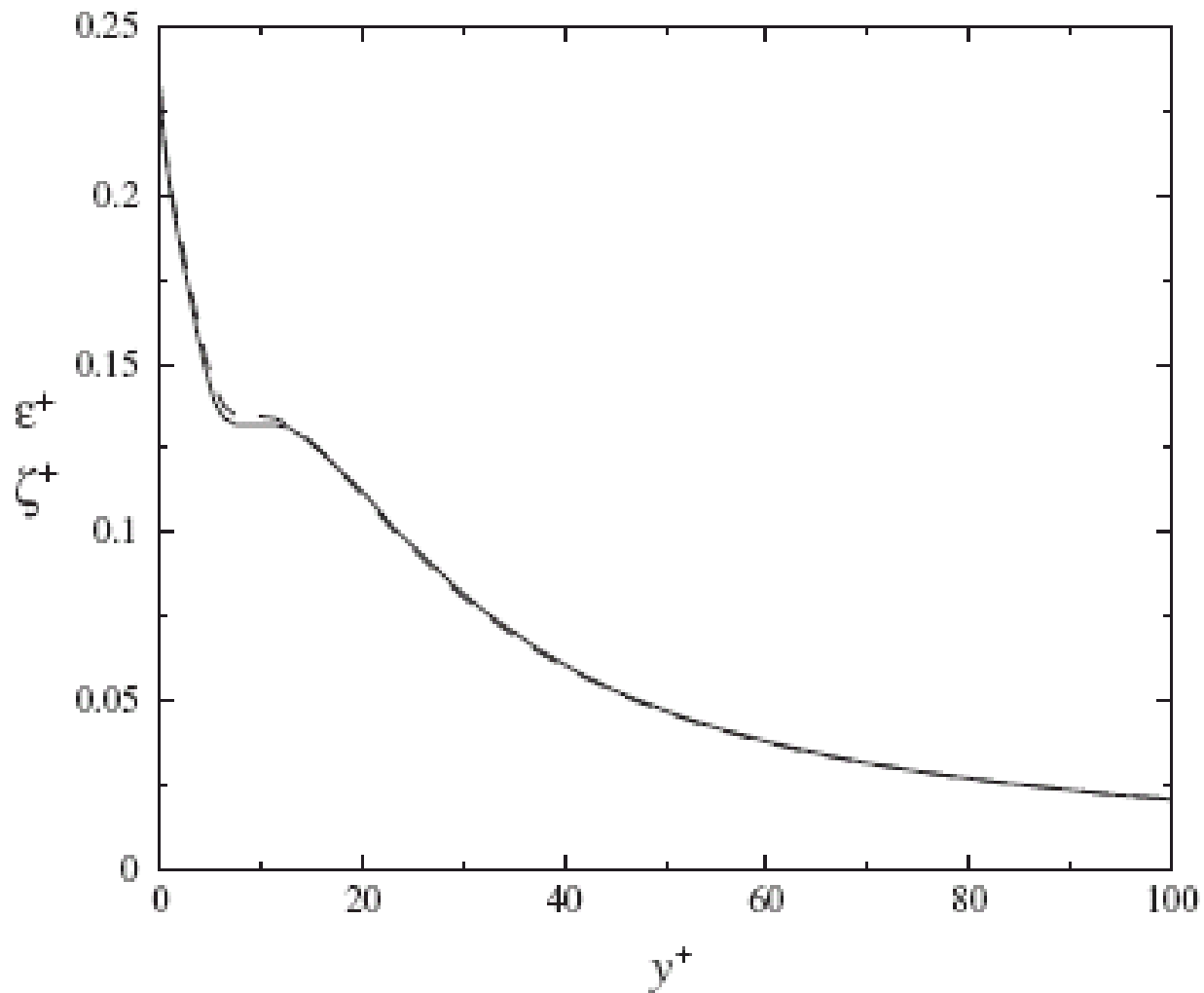


Fig. 4.17 Comparison of enstrophy and kinetic energy dissipation rate in channel flow at $R_\tau = 590$. $--$, ϵ^+ ; $-$, ζ^+ . (From [49].)

Transport equation of mean enstrophy

$$\begin{aligned}
 \frac{\partial}{\partial t} \frac{\overline{\Omega_i \Omega_i}}{2} &+ \underbrace{\frac{\partial}{\partial x_j} \left(\overline{U_j} \frac{\overline{\Omega_i \Omega_i}}{2} \right)}_{\text{Advection}} = - \underbrace{\frac{\partial}{\partial x_j} \left(\overline{\Omega_i \omega_i u_j} \right)}_{\text{Turbulent transport}} + \underbrace{\overline{u_j \omega_i} \frac{\partial \overline{\Omega_i}}{\partial x_j}}_{\text{Production}} + \underbrace{\overline{\Omega_i \Omega_j S_{ij}}}_{\text{Mean stretching}} \\
 &+ \underbrace{\overline{\Omega_i \omega_j s_{ij}}}_{\text{Mixed production}} + \underbrace{\nu \nabla^2 \frac{\overline{\Omega_i \Omega_i}}{2}}_{\text{Viscous diffusion}} - \underbrace{\nu \frac{\partial \overline{\Omega_i}}{\partial x_j} \frac{\partial \overline{\Omega_i}}{\partial x_j}}_{\text{Viscous dissipation}} .
 \end{aligned}$$

Transport equation of fluctuating enstrophy

$$\begin{aligned}
 \frac{\partial}{\partial t} \frac{\overline{\omega_i \omega_i}}{2} &+ \underbrace{\frac{\partial}{\partial x_j} \left(\overline{U_j} \frac{\overline{\omega_i \omega_i}}{2} \right) + \frac{\partial}{\partial x_j} \left(\overline{u_j} \frac{\overline{\omega_i \omega_i}}{2} \right) + \overline{u_j \omega_i} \frac{\partial \overline{\Omega_i}}{\partial x_j}}_{\text{Advection}} = \\
 &+ \underbrace{\overline{\omega_i \omega_j} \frac{\partial \overline{U_i}}{\partial x_j} + \overline{\omega_i \omega_j} \frac{\partial \overline{u_i}}{\partial x_j} + \overline{\Omega_j \omega_i} \frac{\partial \overline{u_i}}{\partial x_j}}_{\text{Rotation and stretching/compression}} \\
 &+ \underbrace{\nu \nabla^2 \frac{\overline{\omega_i \omega_i}}{2}}_{\text{Viscous diffusion}} - \underbrace{\nu \frac{\partial \overline{\omega_i}}{\partial x_j} \frac{\partial \overline{\omega_i}}{\partial x_j}}_{\text{Viscous dissipation}} .
 \end{aligned}$$

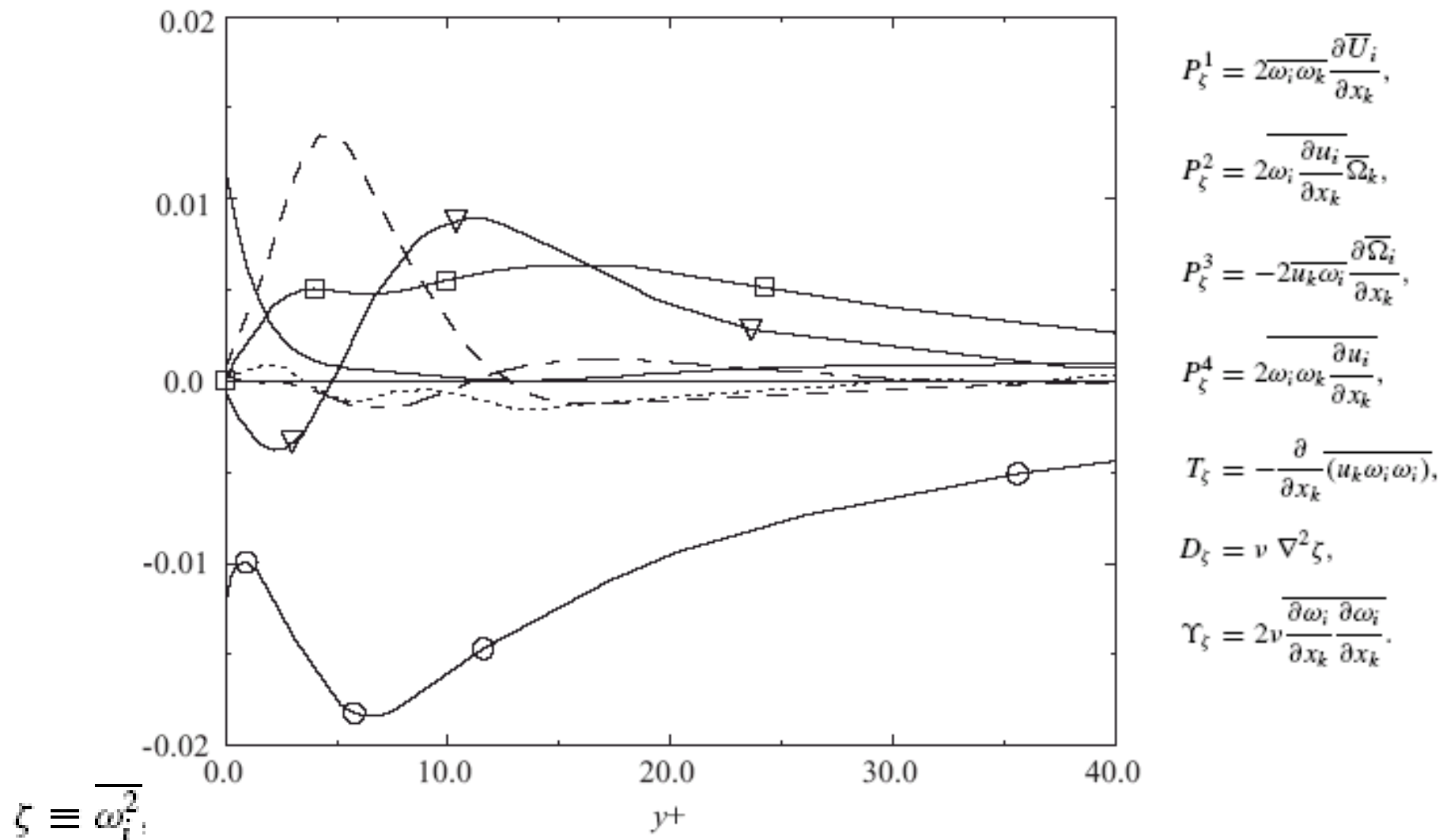


Fig. 4.18 ζ equation budget in channel flow for $R_{\tau} = 145$ scaled with ν and u_{τ} . — —, P_{ζ}^1 ; ∇ , P_{ζ}^2 ; — — —, P_{ζ}^3 ; \square , P_{ζ}^4 ; \cdots , T_{ζ} ; —, D_{ζ} ; \circ , $-\Upsilon_{\zeta}$. (From [23].)

SCALAR TRANSPORT

Diffusion rate in units of scalar/area/sec, $-D \frac{\partial C}{\partial x_j}$

where D is the diffusivity coefficient

Transport equation for a passive scalar

$$\frac{\partial C}{\partial t} + U_j \frac{\partial C}{\partial x_j} = D \nabla^2 C + q$$

Applying Reynolds decomposition and averaging

$$\frac{\partial \bar{C}}{\partial t} + \bar{U}_j \frac{\partial \bar{C}}{\partial x_j} = \frac{\partial}{\partial x_j} \left(D \frac{\partial \bar{C}}{\partial x_j} - \overline{u_i c} \right) + q$$

scalar flux

CORRELATION

Two-point correlation

$$\mathcal{R}_{ij}(\mathbf{x}, \mathbf{y}, t) \equiv \overline{u_i(\mathbf{x}, t)u_j(\mathbf{y}, t)}$$

dividing this by the variances of u_i and u_j gives the correlation coefficient, R_{ij} , which has a limiting maximum value of +1 when $i = j$ and x and y are coincident. It can also take on negative values with a limiting value of -1 when u_i and u_j are the same signals but are 180° out of phase.

Space-time correlations are formed when we let x and y be at different locations and let the time be different for the two variables being correlated.

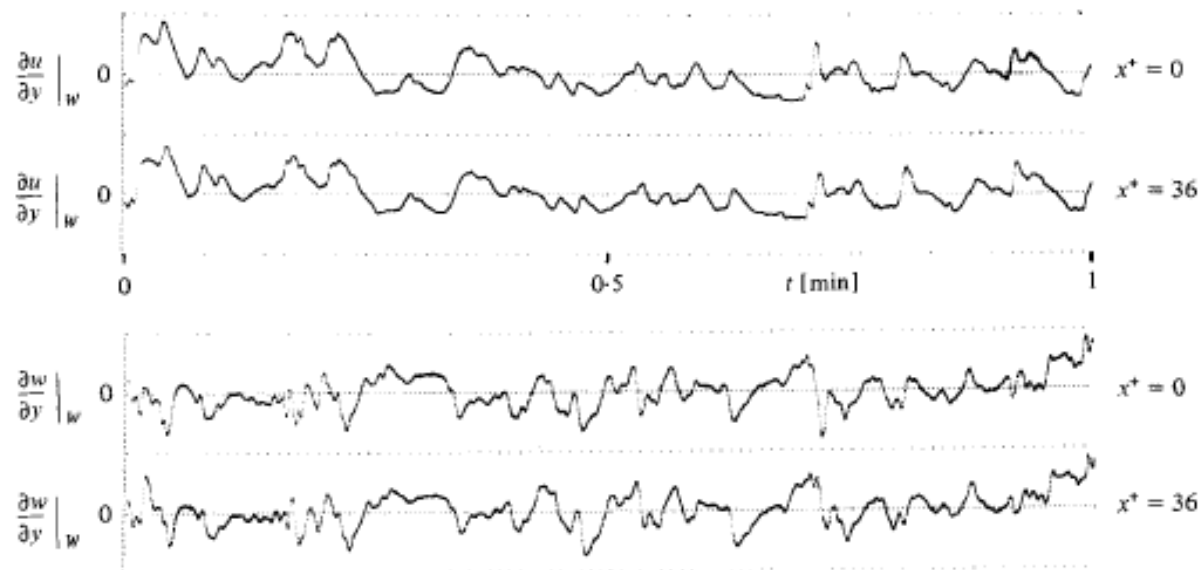


FIGURE 3. Simultaneous records of the fluctuating wall gradients with $\Delta x^+ = 36$, $\Delta z^+ = 0$.

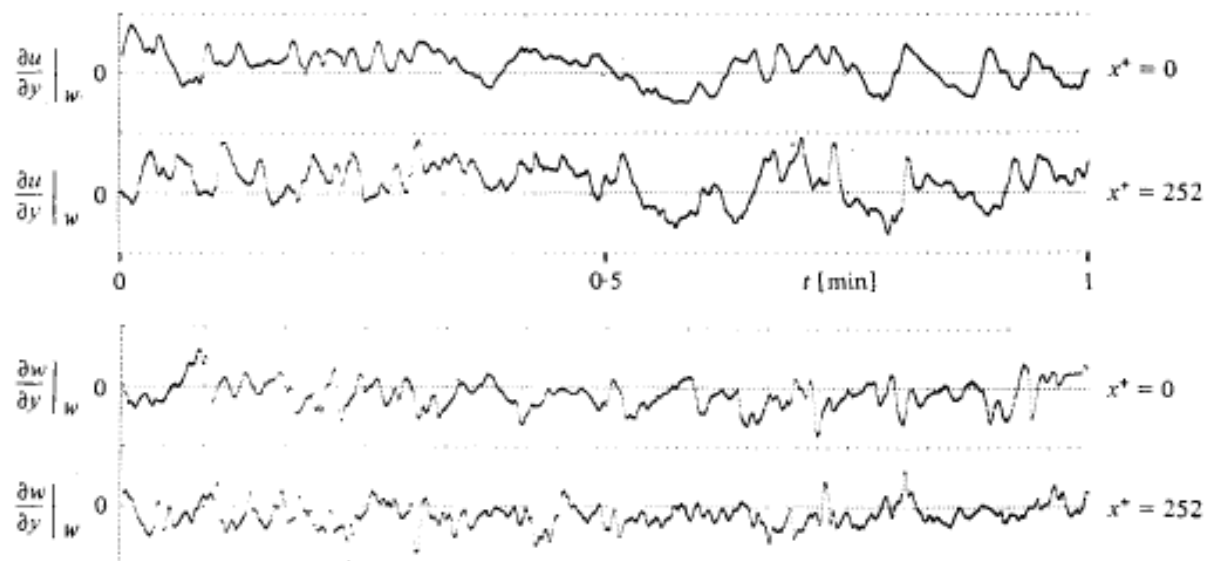


FIGURE 4. Simultaneous records of the fluctuating wall gradients with $\Delta x^+ = 252$, $\Delta z^+ = 0$.

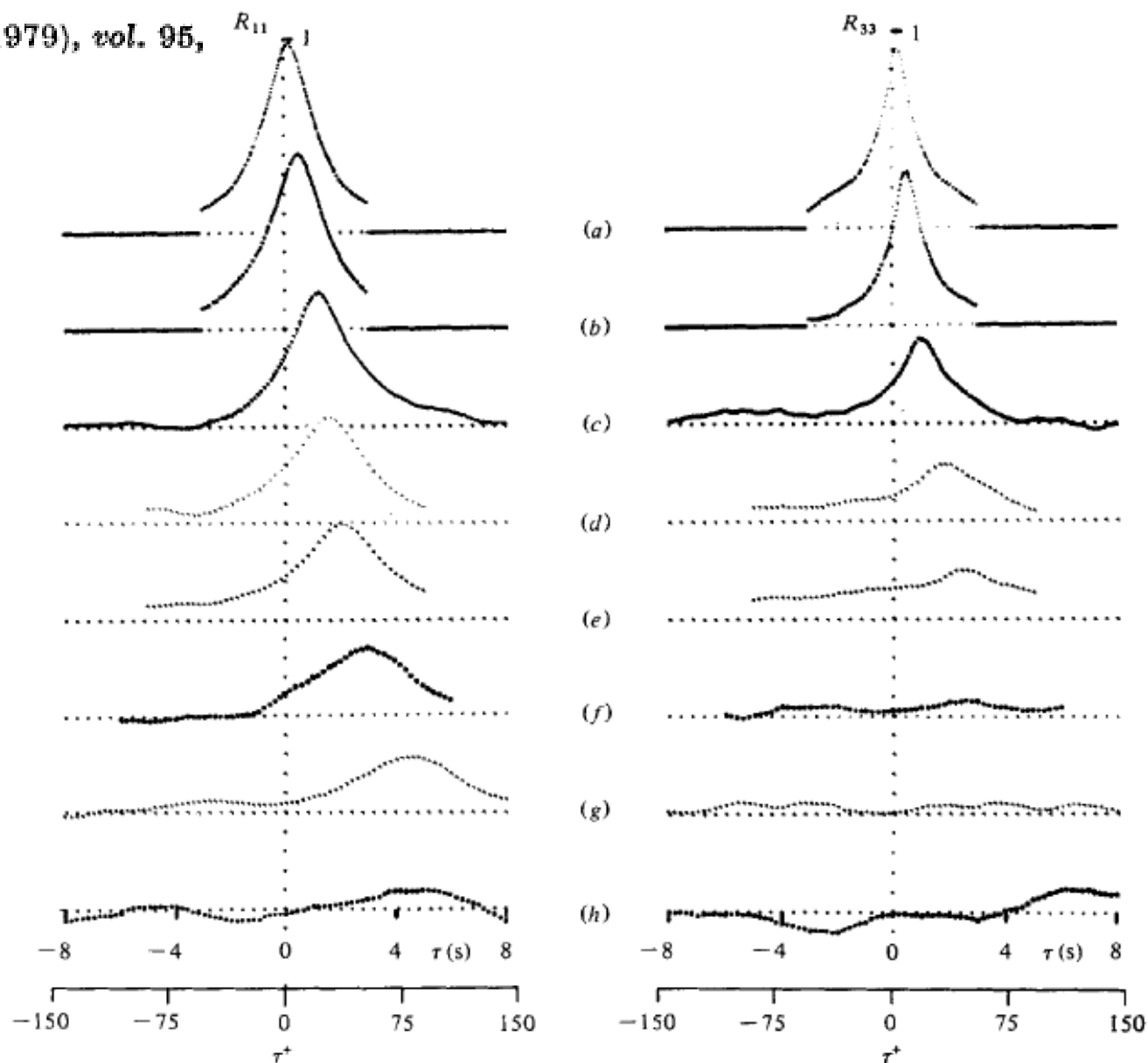


FIGURE 5. Streamwise space-time correlations of $(\partial u/\partial y)|_w$ and $(\partial v/\partial y)|_w$ as a function of Δx^+ . $(\Delta x^+, x/b)$: (a), (36, 0.18); (b), (108, 0.54); (c), (252, 1.3); (d), (378, 1.9); (e), (486, 2.4); (f), (792, 4.0); (g), (1044, 5.2); (h), (1280, 6.4).

SPECTRA

Energy Spectrum Tensor

*Define the separation distance between locations as \underline{r} and take the Fourier transform of the two-point correlation tensor $\mathcal{R}_{ij}(\underline{x}, \underline{x} + \underline{r}, t)$
For a fixed location \underline{x}*

$$E_{ij}(\mathbf{k}, t) \equiv (2\pi)^{-3} \int_{\mathfrak{R}^3} e^{i\mathbf{r}\cdot\mathbf{k}} \mathcal{R}_{ij}(\mathbf{r}, t) d\mathbf{r}.$$

Here \underline{k} is the wavenumber vector. Of course, the inverse Fourier transform is the two-point correlation tensor.

$$\mathcal{R}_{ij}(\mathbf{r}, t) = \int_{\mathfrak{R}^3} e^{-i\mathbf{r}\cdot\mathbf{k}} E_{ij}(\mathbf{k}, t) d\mathbf{k}.$$

*where $d\underline{k} = dk_1 dk_2 dk_3$ is the differential volume in wavenumber space.
Letting $i = j$, $r = 0$ and dividing by 2, yields the spectrum of TKE*

$$K(t) = \frac{1}{2} \int_{\mathfrak{R}^3} E_{ii}(\mathbf{k}, t) d\mathbf{k}.$$

In spherical coordinates this can be written as

$$K(t) = \int_0^{\infty} dk \left[\frac{1}{2} \int_{|\mathbf{k}|=k} d\Omega E_{ii}(\mathbf{k}, t) \right],$$

where $d\Omega$ is an element of solid angle in \mathbf{k} space and $d\mathbf{k} = d\Omega dk$.

The term in brackets is defined as the *energy density function* or, in short, the *energy spectrum*.

$$E(k, t) \equiv \frac{1}{2} \int_{|\mathbf{k}|=k} E_{ii}(\mathbf{k}, t) d\Omega,$$

so that

$$K(t) = \int_0^{\infty} E(k, t) dk.$$

$E(\mathbf{k}, t)$ represents all the energy in a spherical shell in \mathbf{k} -space located at $\mathbf{k} = |\underline{\mathbf{k}}|$.

Time Auto-correlation Function (of a single signal at one location in space correlated with itself as a function of time delay)

$$\mathcal{R}_E(\tau) = \frac{\overline{u(t)u(t + \tau)}}{\overline{u^2(t)}}$$

Integral time scale

$$T_E = \int_{-\infty}^{\infty} \mathcal{R}_E(\tau) d\tau$$

The Fourier transform of $\mathcal{R}_E(\tau)$ is

$$\widehat{\mathcal{R}}_E(\omega') = \int_{-\infty}^{\infty} e^{-i\tau\omega'} \mathcal{R}_E(\tau) d\tau$$

where $\omega' = 2\pi \omega$ is the angular frequency (radians) and ω is the frequency (rev/s).

The inverse transform is, of course, the time auto-correlation function itself

$$\mathcal{R}_E(\tau) = \frac{1}{2\pi} \int_{-\infty}^{\infty} e^{i\tau\omega'} \widehat{\mathcal{R}}_E(\omega') d\omega'$$

Evaluating $\mathcal{R}_E(\tau)$ at $\tau = 0$ and defining

$$E_{11}(\omega) = 2\overline{u^2} \widehat{\mathcal{R}}_E(2\pi\omega)$$

after a change of variable we have

$$\overline{u^2} = \frac{1}{2} \int_{-\infty}^{\infty} E_{11}(\omega) d\omega.$$

If $\mathcal{R}_E(\tau)$ is symmetric $\overline{u^2} = \int_0^{\infty} E_{11}(\omega) d\omega.$

E_{11} is called the frequency spectrum. It can easily be determined From time series of experimental data.

For isotropic turbulence $R_{11}(\underline{r}, t)$ can be related to $\mathcal{R}_E(\tau)$ by means of “Taylor’s Hypothesis, and $E(\underline{k}, t)$ can be calculated from $E_{11}(\omega)$.

Taylor's Frozen Turbulence Hypothesis
to determine streamwise gradients

$$\frac{dU_i}{dx} = -\frac{1}{U_c} \frac{dU_i}{dt}$$

Alternatively, setting the acceleration equal to zero in the N-S equations

$$\frac{\partial U_i}{\partial t} + U_1 \frac{\partial U_i}{\partial x} + U_2 \frac{\partial U_i}{\partial y} + U_3 \frac{\partial U_i}{\partial z} = 0.$$

Rearranging (3.31) yields

$$\frac{\partial U_i}{\partial x} = -\frac{1}{U_1} \left(\frac{\partial U_i}{\partial t} + U_2 \frac{\partial U_i}{\partial y} + U_3 \frac{\partial U_i}{\partial z} \right).$$

Streamwise wavenumber approximated from frequency

$$k_x \approx \frac{2\pi f}{U_1}$$

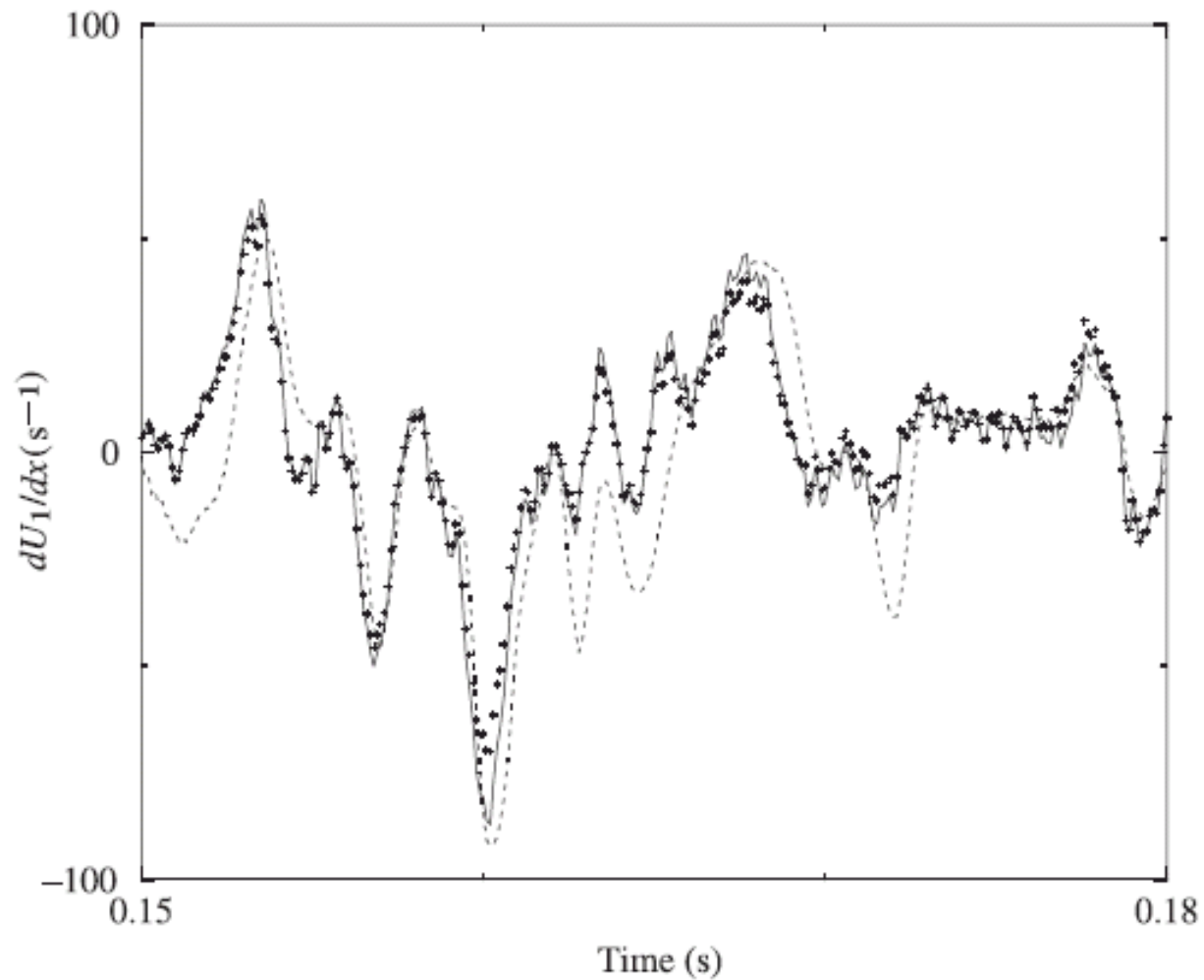


Fig. 3.5 Comparison of time-series signals determined from Taylor's hypothesis [Eqs. (3.30) — and (3.32) +++] and from the continuity equation (· · ·) using mixing-layer data from a 12-sensor probe. (From [31].)

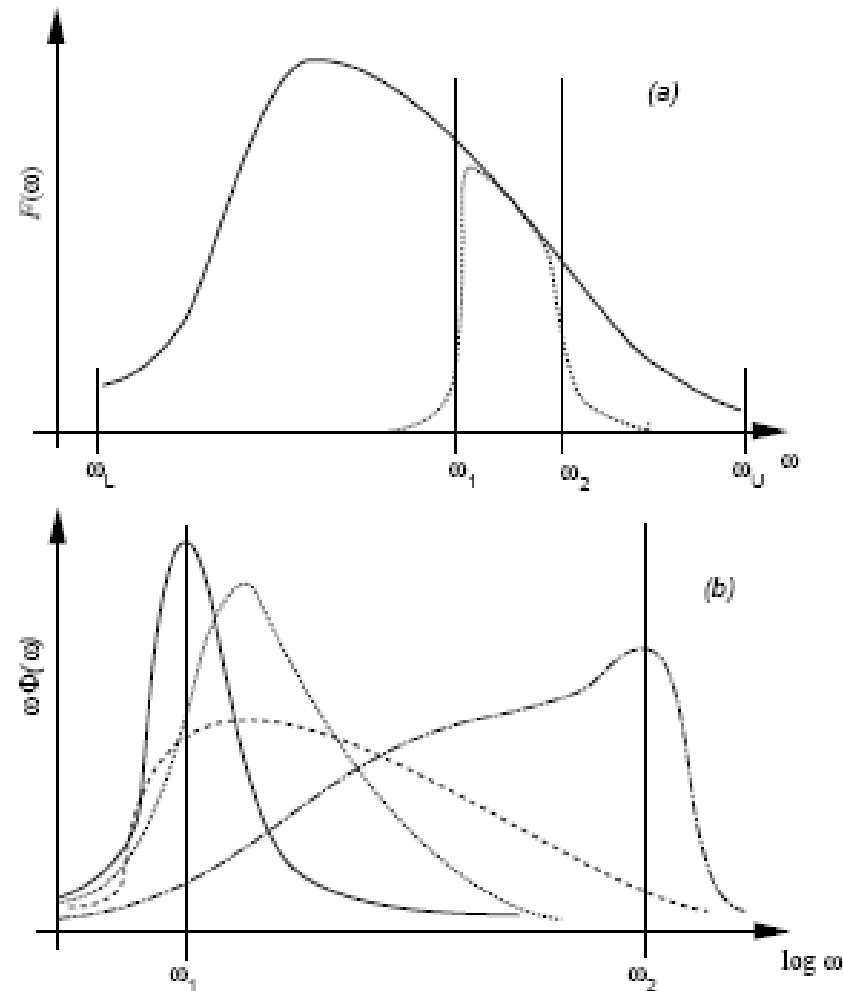


Figure 5.1: Frequency spectra. (a) Development of a frequency spectrum from narrow-band elements: contribution of a filter with nominal limits ω_1 and ω_2 ; — complete power spectrum. (b) Sketch of the weighted (by ω) frequency spectra for: — Reynolds shear stress $\overline{u'v'}$, streamwise velocity fluctuations u , --- pressure fluctuations p' and - · - · - approximation of dissipation rate $\overline{(\partial u / \partial t)^2}$ (from AJR [?]).

$$\mathbf{k}_1 = 2\pi\omega/U_C$$

$$\omega = \mathbf{k}_1 U_C / 2\pi$$

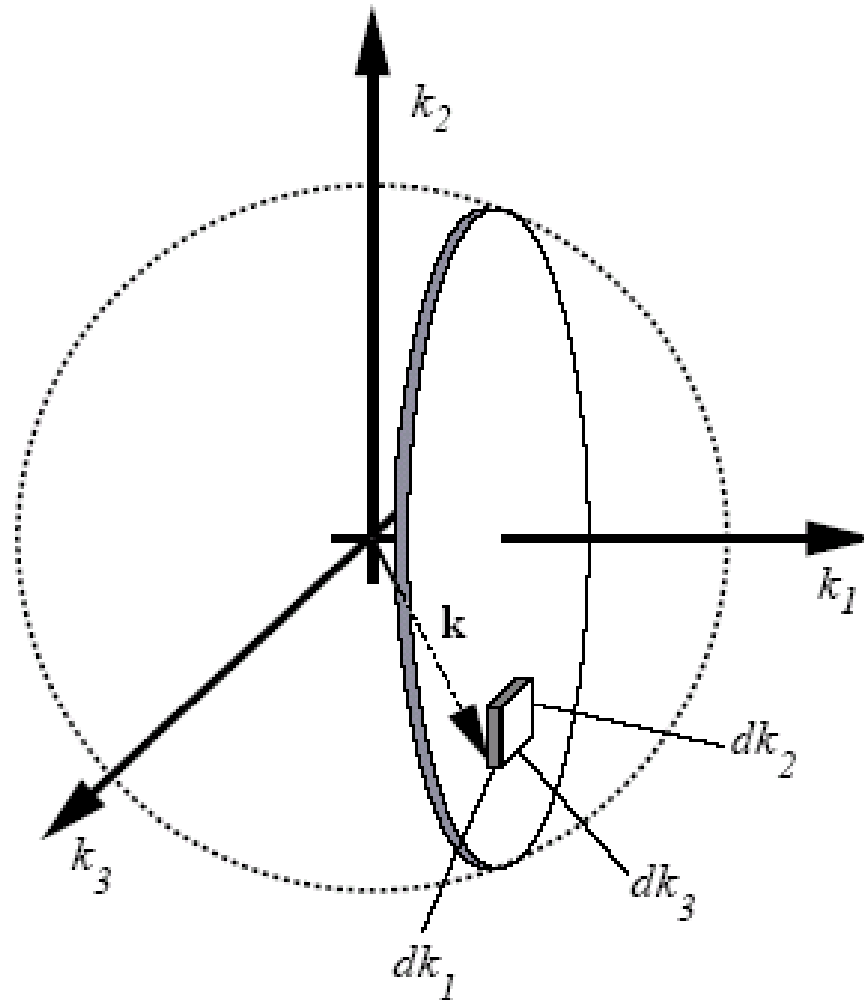


Figure 5.2: One-dimensional and three-dimensional spectra (from Bradshaw [?]).

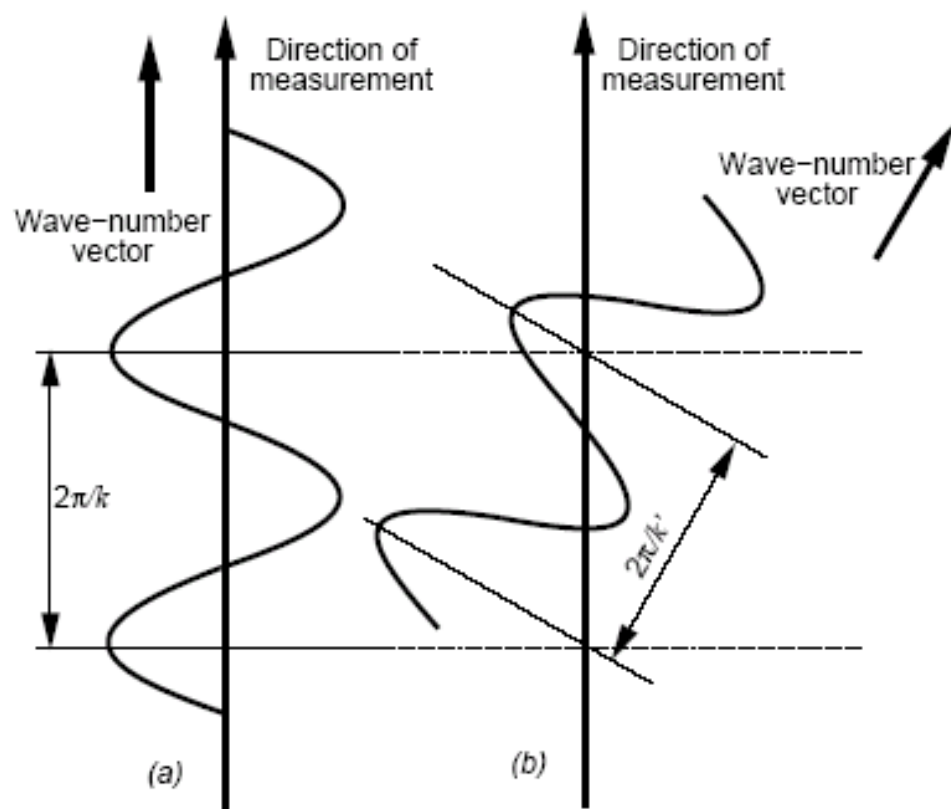


Figure 5.3: Aliasing in a one-dimensional spectrum: (a) a wave of true wave-number k , aligned with the line of measurement, (b) a wave of wave-number $k' > k$, with wave-number vector oblique to the line of measurement (from TL [?]).

TURBULENCE SCALES

Smallest scales of turbulence are in a state of *universal equilibrium*, according to Kolmogorov, that should depend only on the rate of dissipation, ϵ , and the viscosity, ν

Kolmogorov length scale $\eta \equiv \frac{\nu^{3/4}}{\epsilon^{1/4}}$

Kolmogorov time scale $t_d = \left(\frac{\nu}{\epsilon}\right)^{1/2}$

Kolmogorov velocity scale $v_d = (\nu\epsilon)^{1/4}$

Isotropic dissipation rate, $\epsilon(t) = \nu \int_0^\infty k^2 E(k, t) dk$

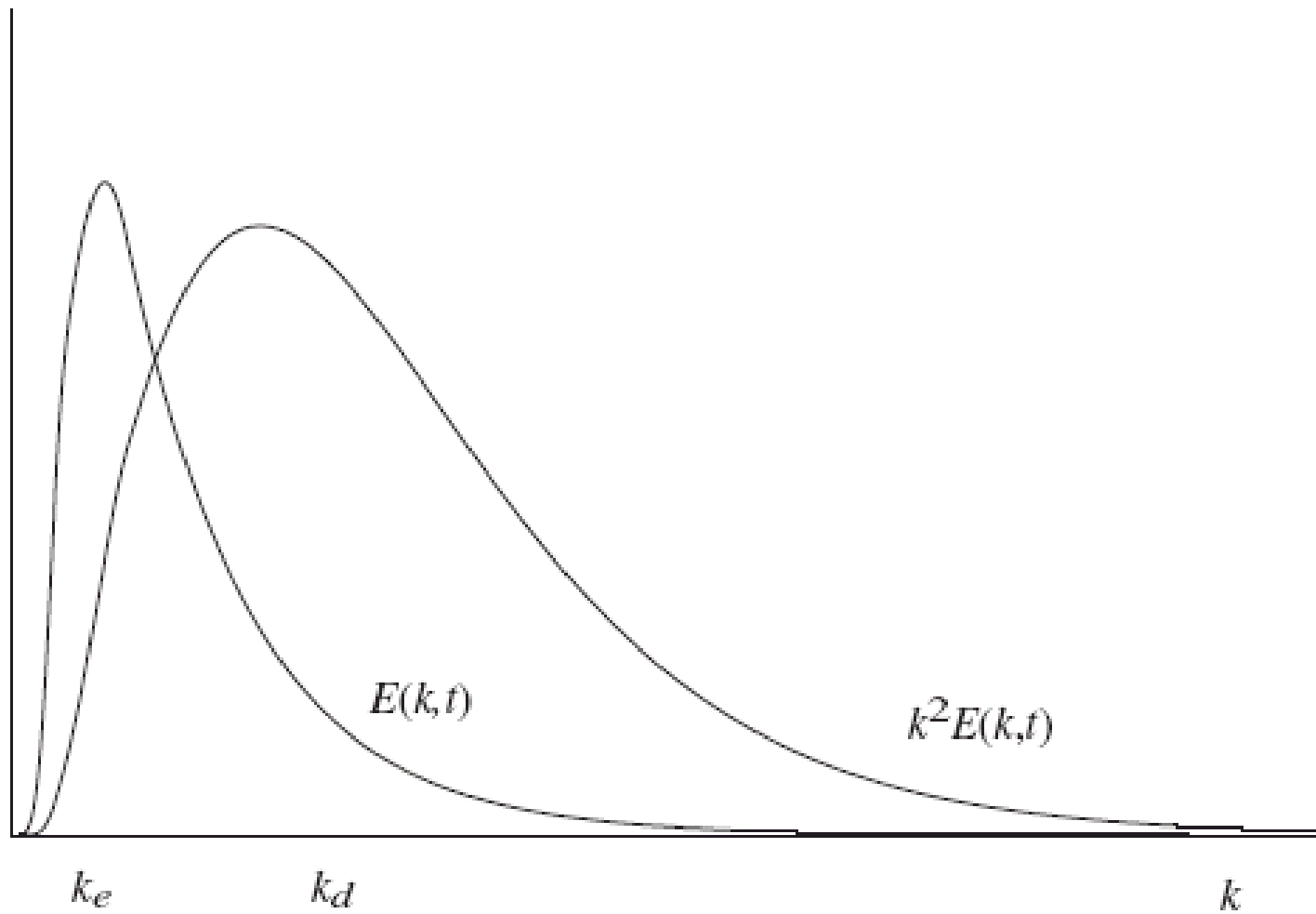


Fig. 2.2 Spectral ranges of $E(k, t)$ and $k^2 E(k, t)$.

Eulerian integral time scale

From the auto-correlation coefficient

$$R(\tau) = \frac{\overline{s(t)s(t+\tau)}}{\overline{s^2}},$$

we can define the *Eulerian integral time scale* as

$$T_E = \int_0^\infty R(\tau) d\tau.$$

Eulerian temporal micro-scale

$$\tau_E = \left[\frac{2\overline{s^2}}{(\partial s / \partial t)^2} \right]^{\frac{1}{2}},$$

Eulerian integral length- and micro-length scales

$$R(r) = \frac{\overline{s(\mathbf{x})s(\mathbf{x}+\mathbf{r})}}{\overline{s^2}}, \quad L_e = \int_0^\infty R(r) dr$$

$$\lambda = \left[-\frac{2}{\partial R(0) / \partial r^2} \right]^{\frac{1}{2}} = \left[\frac{2\overline{s^2}}{(\partial s / \partial r)^2} \right]^{\frac{1}{2}} \quad \lambda_{x_1} = \frac{\lambda_{11}}{\sqrt{2}} = \left[\frac{\overline{u_1^2}}{(\partial u_1 / \partial x_1)^2} \right]^{\frac{1}{2}}$$

Taylor micro-scale (named after G. I. Taylor)

Two spatial correlations that play a special role in *isotropic* turbulence theory and are found from $R_{ij}(\underline{r}, t)$ are longitudinal and transverse correlation functions

$$\overline{u_1^2} f(r) \equiv \mathcal{R}_{11}(r\mathbf{e}_1, t) \quad \overline{u_2^2} g(r) \equiv \mathcal{R}_{22}(r\mathbf{e}_1, t)$$

where \underline{e}_i is the unit vector in the coordinate direction.

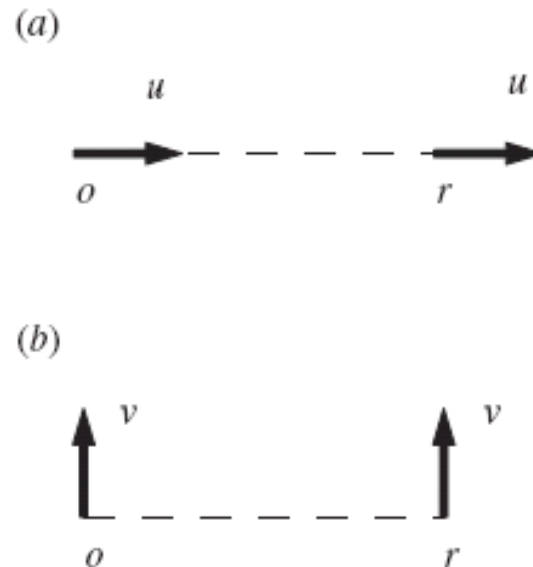


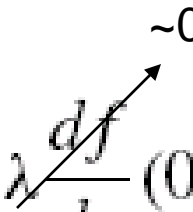
Fig. 1.4 (a) Longitudinal and (b) transverse velocity correlations used in definitions of $f(r)$ and $g(r)$, respectively.

Micro length-scale

Defined from Taylor series of $f(r)$ near $r = 0$. It is a measure of the scales at which turbulent dissipation occurs.

$$f(r) = 1 + r \frac{df}{dr}(0) + \frac{r^2}{2!} \frac{d^2 f}{dr^2}(0) + \dots$$

So for $f = 0$, $r = \lambda$

$$0 = 1 + \lambda \frac{df}{dr}(0) + \frac{\lambda^2}{2!} \frac{d^2 f}{dr^2}(0).$$


The microscale, λ , is the intercept of this parabola with the r -axis. It is obviously related to the curvature of f at $r = 0$.

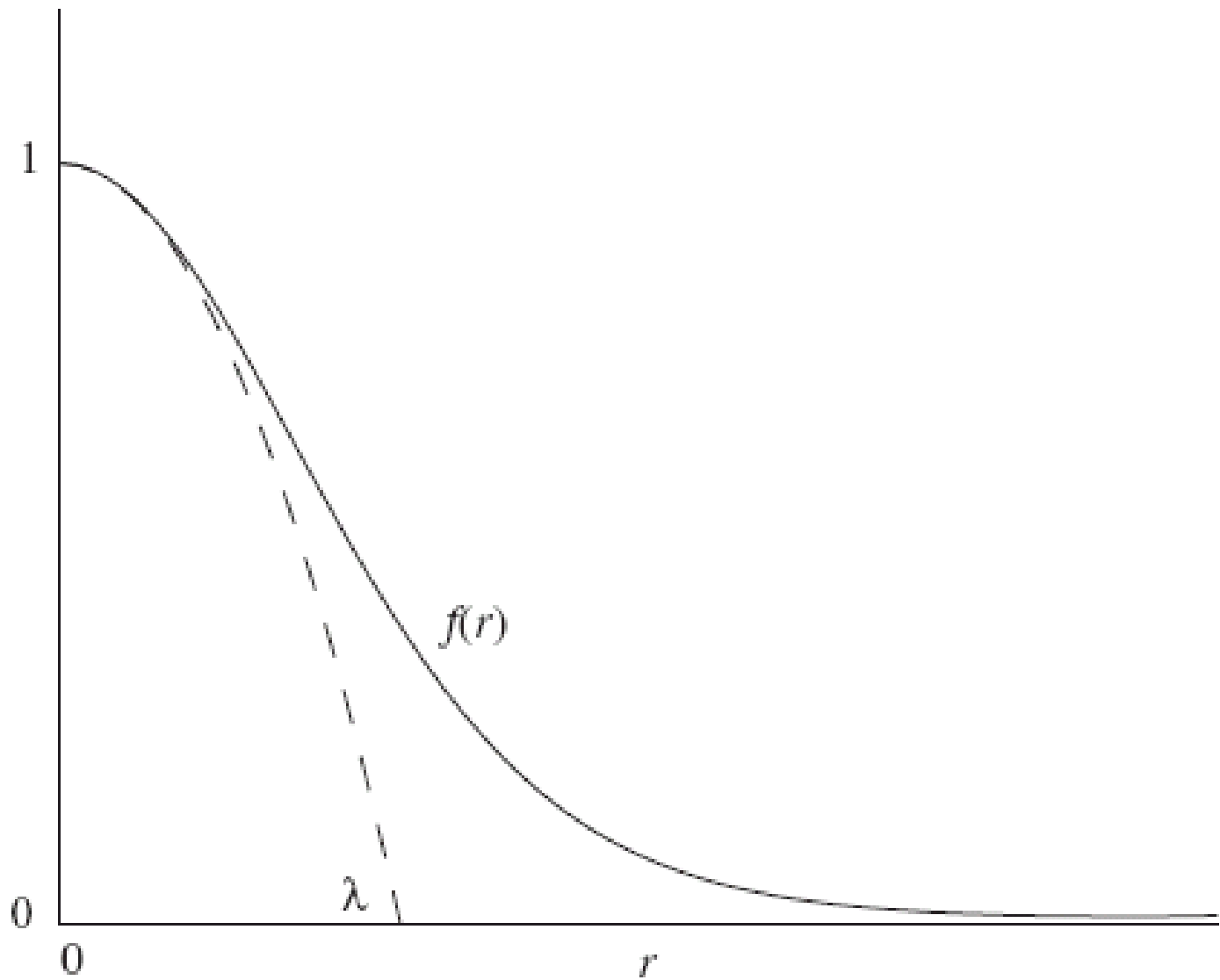


Fig. 1.5 Microscale definition.

Ratios of Scales

For isotropic turbulence

$$\frac{L_e}{\lambda} \sim R_\lambda, \quad \text{where } R_\lambda = u_{\text{rms}}\lambda/\nu \text{ is a turbulence Reynolds number.}$$

Choosing a different Reynolds number, $R_e = u_{\text{rms}}l_e/\nu$

based on the physical size of the flow domain and from the definition of η

$$\frac{\eta}{\lambda} \sim \frac{1}{\sqrt{R_\lambda}} \sim \frac{1}{R_e^{1/4}}, \quad (2.101)$$

showing that η is generally smaller than λ but not so much so. In fact it can be seen that λ is a reasonable measure of the scales where most of the dissipation takes place.

$$\frac{L_e}{\eta} \sim R_\lambda^{3/2} \sim R_e^{3/4}, \quad (2.102)$$

which is the ratio of the largest to smallest scales in the flow.

A three-dimensional mesh would then have to be $\sim (l_e/\eta)^3$ in size. In view of (2.102) it follows that the number of mesh points in a fully resolved turbulent flow simulation has a $R_e^{9/4}$ dependence on Reynolds number.

Inertial Subrange

Range of scales over which there is no significant kinetic energy production or dissipation and where the energy spectrum depends only on the dissipation rate, ϵ , and not on the viscosity. This is the idea of the “energy cascade.” Dimensionally this requires that the spectrum have the form

$$E(k, t) \sim k^{-5/3} \epsilon^{2/3},$$

or with a Kolmogorov constant C_K ,

$$E(k, t) = C_K k^{-5/3} \epsilon^{2/3}.$$

The one-dimensional spectrum also has a $k^{-5/3}$ dependency.

assuming isotropy, the one-dimensional longitudinal and transverse spectra

$$\begin{aligned} E_{11}(k_1) &= C_1 \epsilon^{1/3} k_1^{-5/3} & C &= 55/18 \quad C_1 \sim 3 \\ E_{22}(k_1) &= E_{33}(k_1) = C'_1 \epsilon^{1/3} k_1^{-5/3} & C_1 &\approx 0.49 \quad C'_1 \approx 0.65 \end{aligned}$$

respectively. The Kolmogorov constant C is equal to $\frac{55}{18}C_1$ (Monin & Yaglom 1940) evaluated in the inertial subrange gives $C'_1/C_1 = 4/3$. and

$$E_{22}(k_1) = E_{33}(k_1) = \frac{1}{2} \left(1 - k_1 \frac{\partial}{\partial k_1} \right) E_{11}(k_1)$$

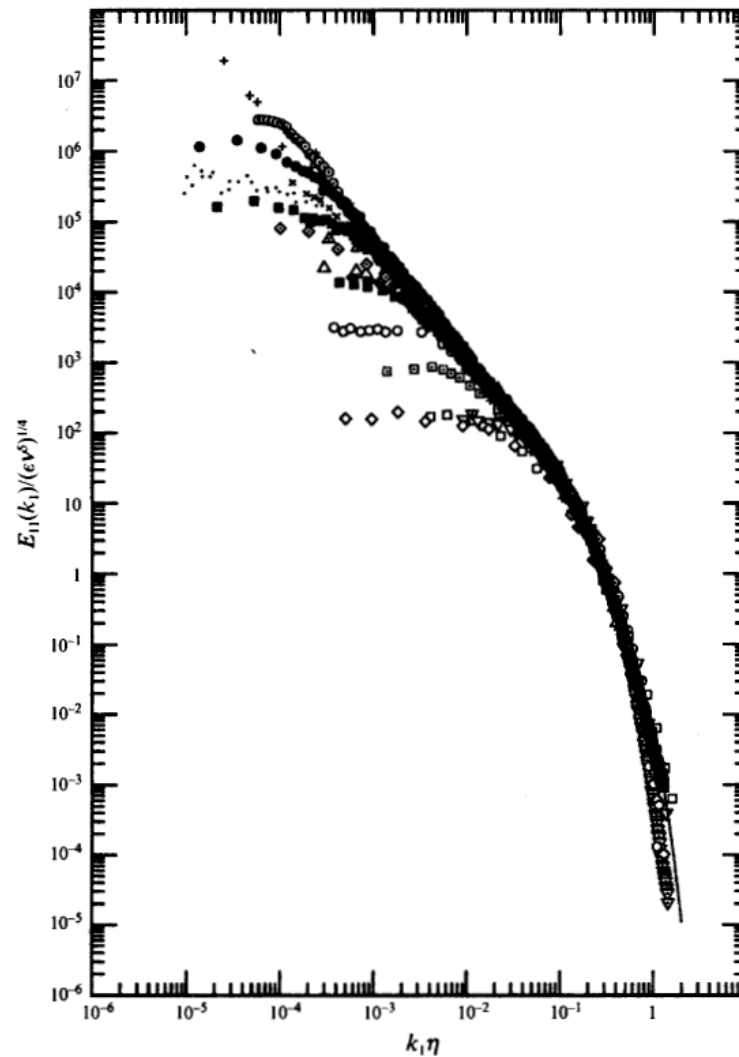
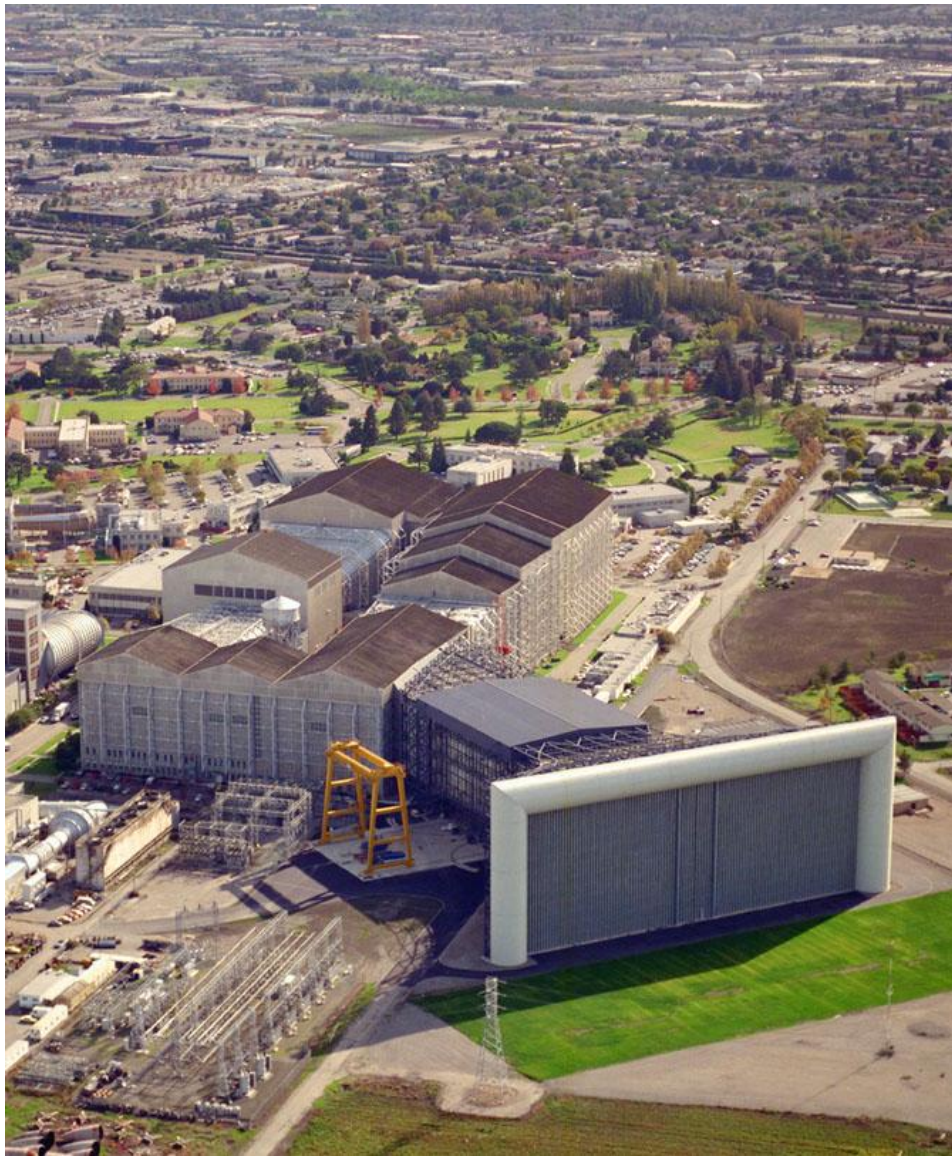


FIGURE 9. Kolmogorov's universal scaling for one-dimensional longitudinal power spectra. The present mid-layer spectra for both free-stream velocities are compared with data from other experiments. This compilation is from Chapman (1979), with later additions. The solid line is from Pao (1965). R_s : \square , 23 boundary layer (Tielman 1967); \diamond , 23 wake behind cylinder (Uberoi & Freymuth 1969); ∇ , 37 grid turbulence (Comte-Bellot & Corrsin 1971); ∇ , 53 channel centreline (Kim & Antonia (DNS) 1991); \square , 72 grid turbulence (Comte-Bellot & Corrsin 1971); \circ , 130 homogeneous shear flow (Champagne *et al.* 1970); \boxtimes , 170 pipe flow (Laufer 1954); \oplus , 282 boundary layer (Tielman 1967); \diamond , 308 wake behind cylinder (Uberoi & Freymuth 1969); \triangle , 401 boundary layer (Sanborn & Marshall 1965); \triangle , 540 grid turbulence (Kistler & Vrebalovich 1966); \times , 780 round jet (Gibson 1963); \cdot , 850 boundary layer (Coantic & Favre 1974); $+$, ~ 2000 tidal channel (Grant *et al.* 1962); \circ , 3180 return channel (CAHI Moscow 1991); \bullet , 1500 boundary layer (present data, mid-layer: $U_e = 50 \text{ m s}^{-1}$); \blacksquare , 600 boundary layer (present data, mid-layer: $U_e = 10 \text{ m s}^{-1}$).



Local isotropy

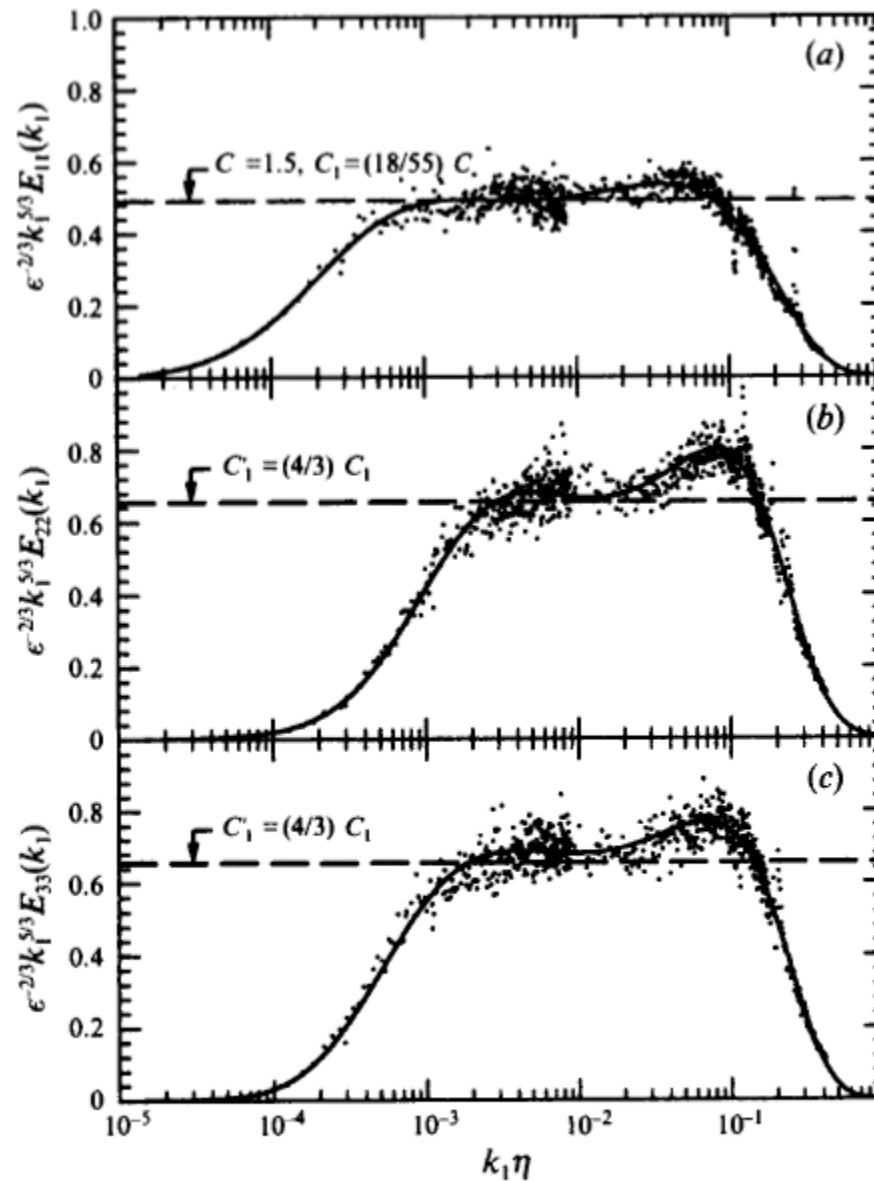


FIGURE 13. Compensated longitudinal and transverse spectra measured at mid-layer for the high-speed case ($y = 400$ mm, $y^+ \approx 62000$, $R_\lambda \approx 1450$). Only the data for wavenumber range $k_1 \eta < 0.25$ can be accepted. Solid lines are the ninth-order, least-square, log-log polynomial fits to the spectral data. (a) u_1 -spectrum; (b) u_2 -spectrum; (c) u_3 -spectrum.

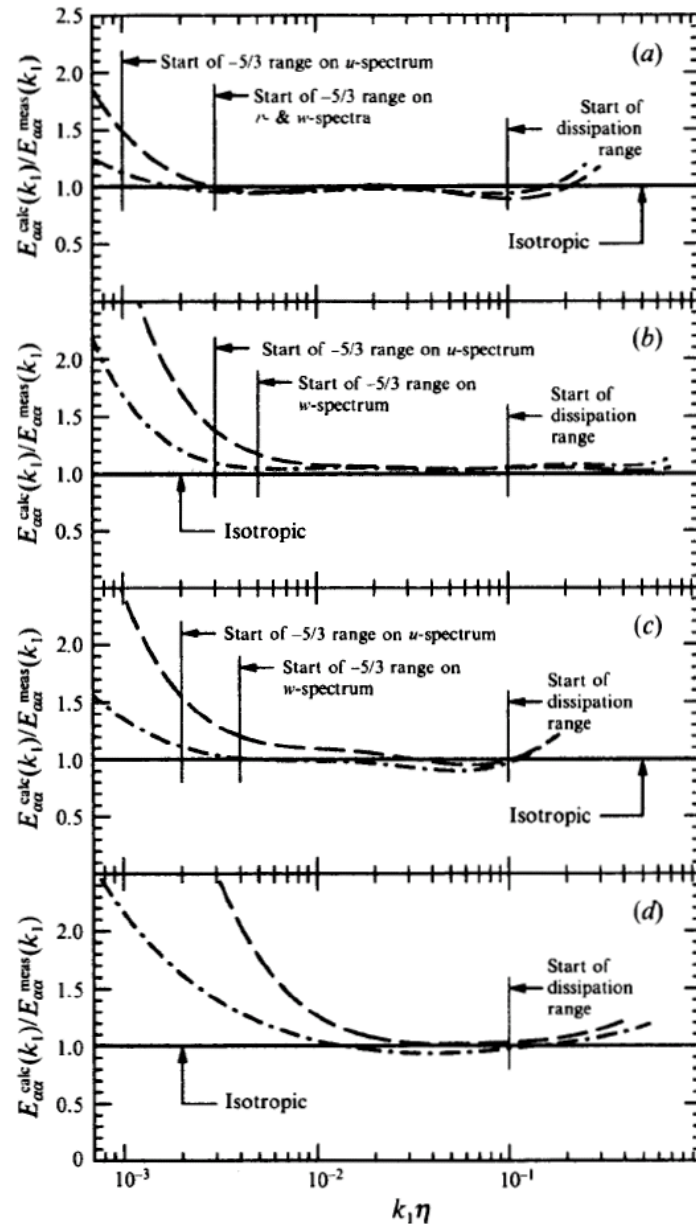


FIGURE 22. Ratios of the calculated to measured transverse spectra at different locations in the boundary layer for two different free-stream velocities. ---, $\alpha = 2$; - · -, $\alpha = 3$. For key to captions for (a)–(d) see figure 20.

Local isotropy in turbulent boundary layers

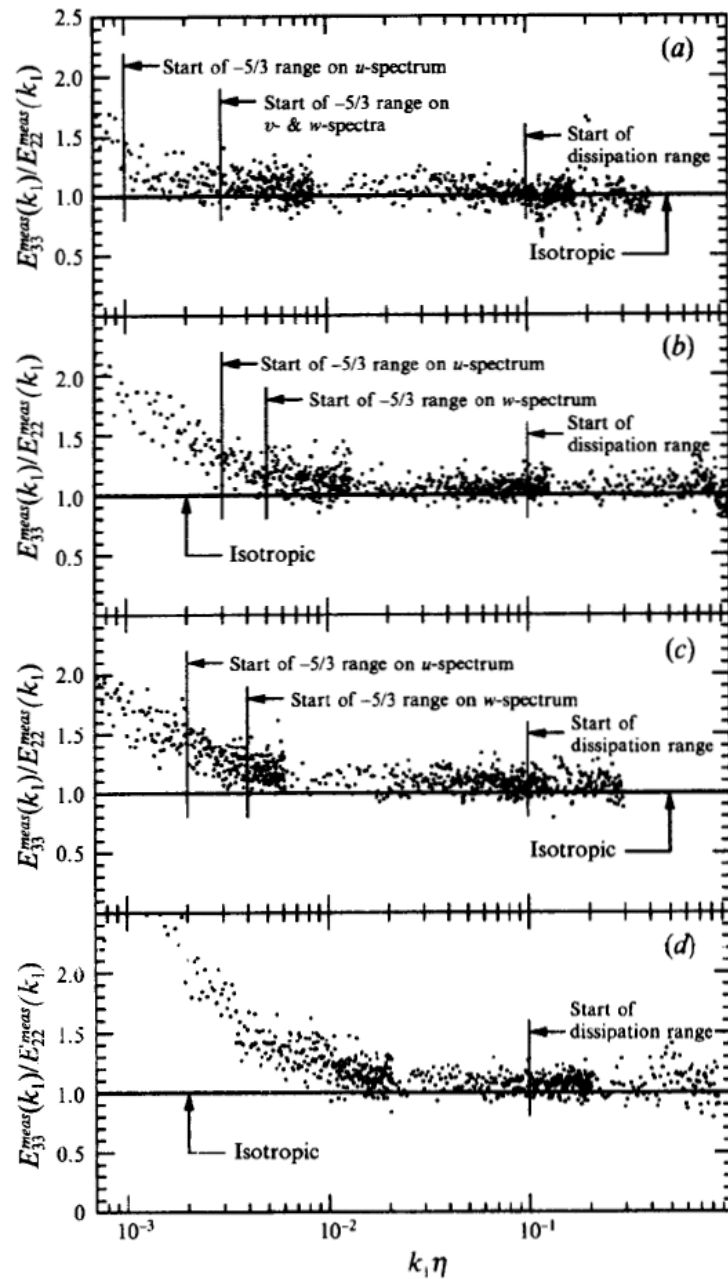


FIGURE 21. Ratios of the measured u_3 -spectra to u_2 -spectra at different locations in the bound layer for two different free-stream velocities. For key to captions for (a)–(d) see figure 20.

PROBABILITY DENSITY FUNCTIONS & CENTRAL MOMENTS

$$P(S) = \lim_{T \rightarrow \infty} \lim_{\Delta S \rightarrow 0} \frac{\sum \Delta t}{T \Delta S} \quad S = \bar{S} + s_i$$

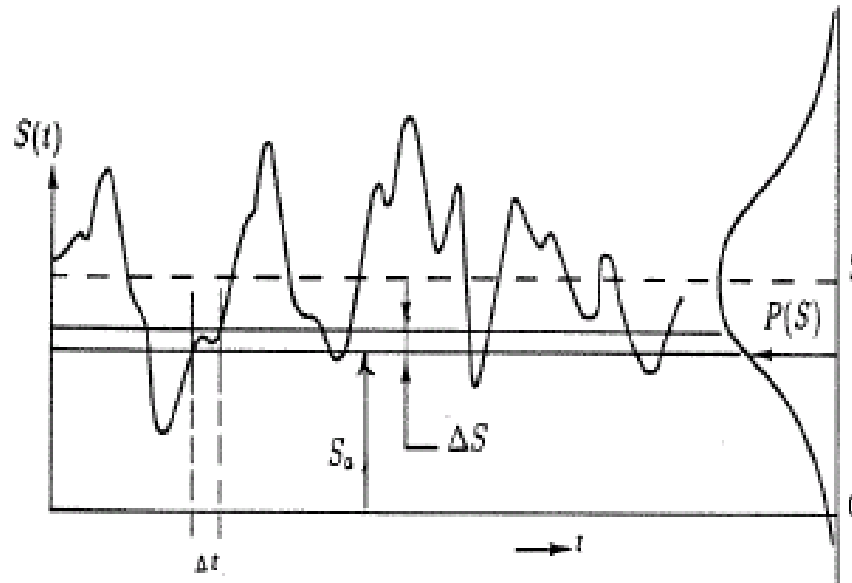


Figure 4.1: Sketch of how the probability density function (PDF) is determined from a time series of a signal $S(t)$ (from TL [113]).

$$\int_{-\infty}^{\infty} P(S) dS = 1$$

Mean value of S $\bar{S}(t) \equiv \lim_{T \rightarrow \infty} \frac{1}{T} \int_{t_0}^{t_0+T} S(t) dt = \int_{-\infty}^{\infty} S P(S) dS.$

n^{th} moment of S $\bar{S}^n = \int_{-\infty}^{\infty} S^n P(S) dS.$

n^{th} moment of Fluctuation s $\bar{s}^n = \int_{-\infty}^{\infty} s^n P(s) ds$

Skewness factor $\mathcal{S}(s) \equiv \frac{\bar{s}^3}{\sigma^3} = \frac{1}{\sigma^3} \int_{-\infty}^{\infty} s^3 P(s) ds$

with σ the standard deviation (rms) of s

Flatness factor (Kurtosis) $\mathcal{F}(s) \equiv \frac{\bar{s}^4}{\sigma^4} = \frac{1}{\sigma^4} \int_{-\infty}^{\infty} s^4 P(s) ds,$

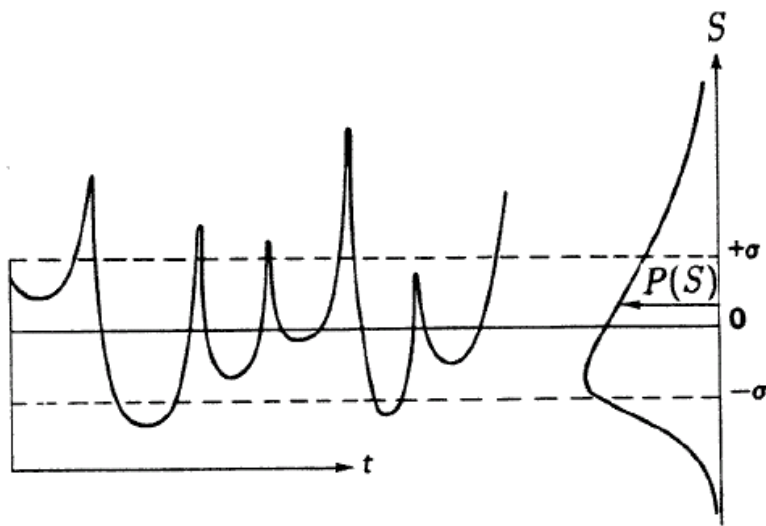


Figure 4.2: The PDF of a positively skewed time series $S(t)$ (from TL [113])

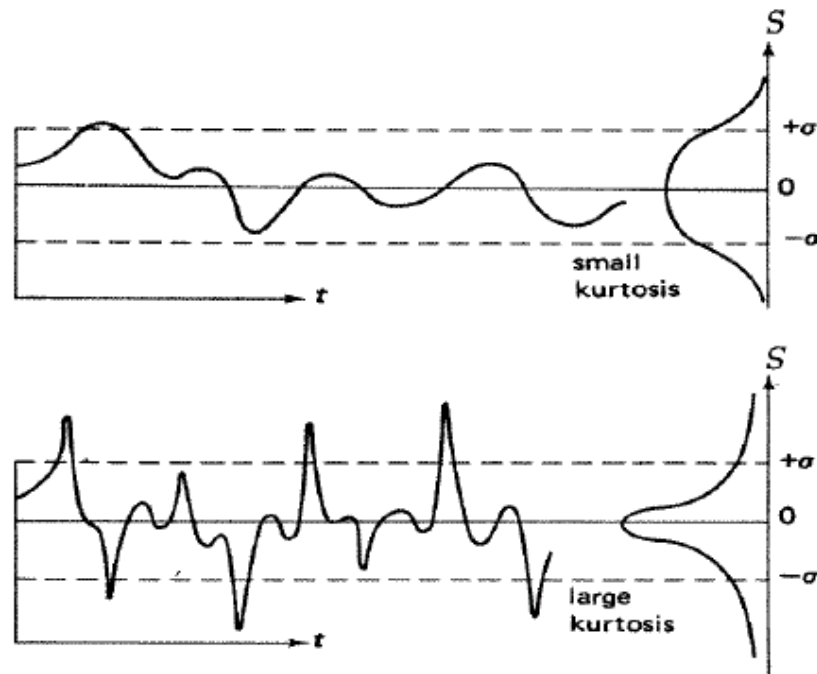


Figure 4.3: Examples of the PDFs of two time series $S(t)$ that have small and large flatness factors (from TL [113]).

Joint Probability Densities and statistical independence

$$\mathbf{JPDF} \quad P(S_1, S_2) = \lim_{T \rightarrow \infty} \lim_{\substack{\Delta S_1 \rightarrow 0 \\ \Delta S_2 \rightarrow 0}} \frac{\sum \Delta t}{T \Delta S_1 \Delta S_2}$$

$$P(S_1, S_2) \geq 0 \quad \text{and} \quad \int_{-\infty}^{\infty} \int_{-\infty}^{\infty} P(S_1, S_2) dS_1 dS_2 = 1$$

$$\mathbf{Joint Moment} \quad \overline{S_1 S_2} = \int_{-\infty}^{\infty} \int_{-\infty}^{\infty} S_1 S_2 P(S_1, S_2) dS_1 dS_2$$

$$\mathbf{Statistical independence when} \quad P(S_1, S_2) = P_{S_1}(S_1)P_{S_2}(S_2)$$

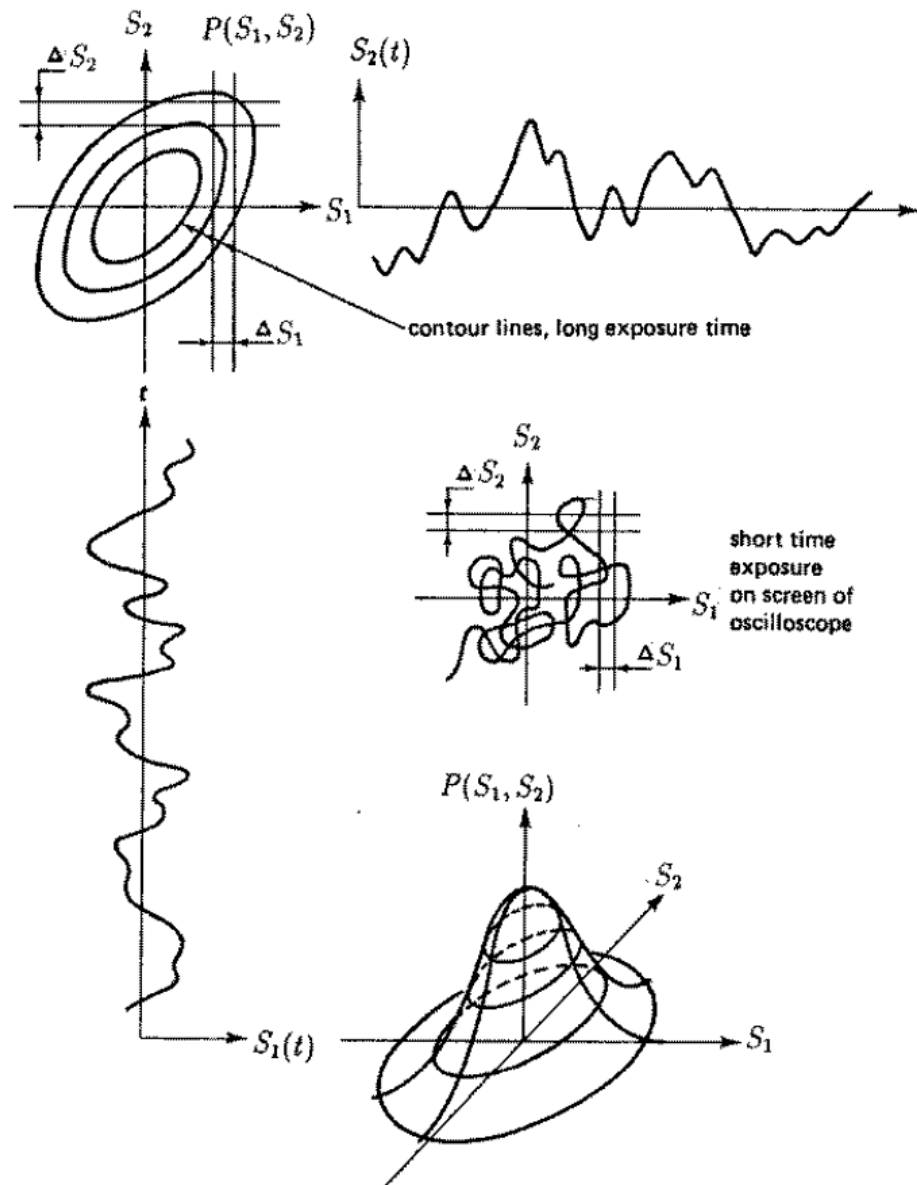
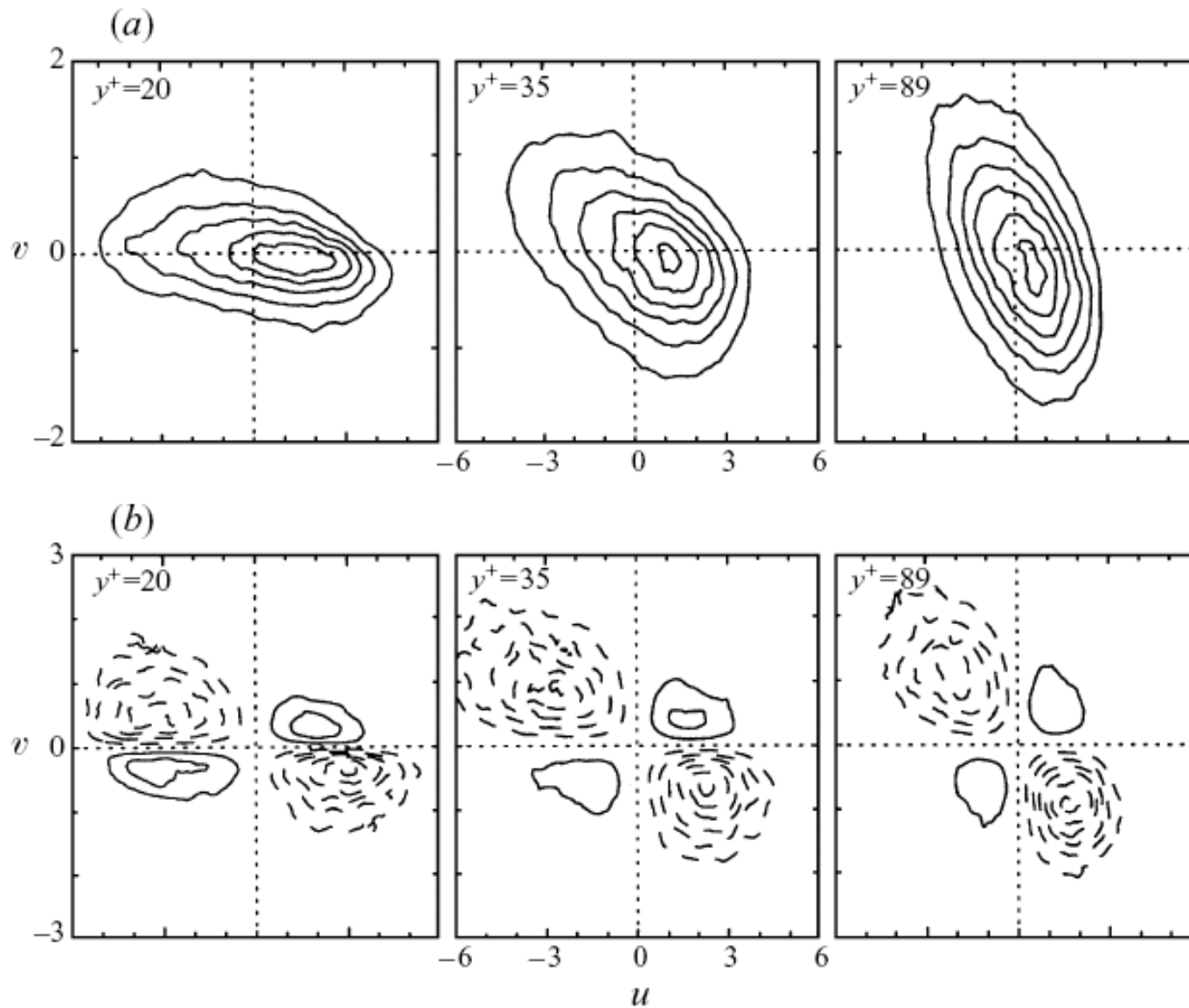


Figure 4.4: Sketch of how the joint probability density function (JPDF) is determined from two time series $S_1(t)$ and $S_2(t)$ (from TL [113]).



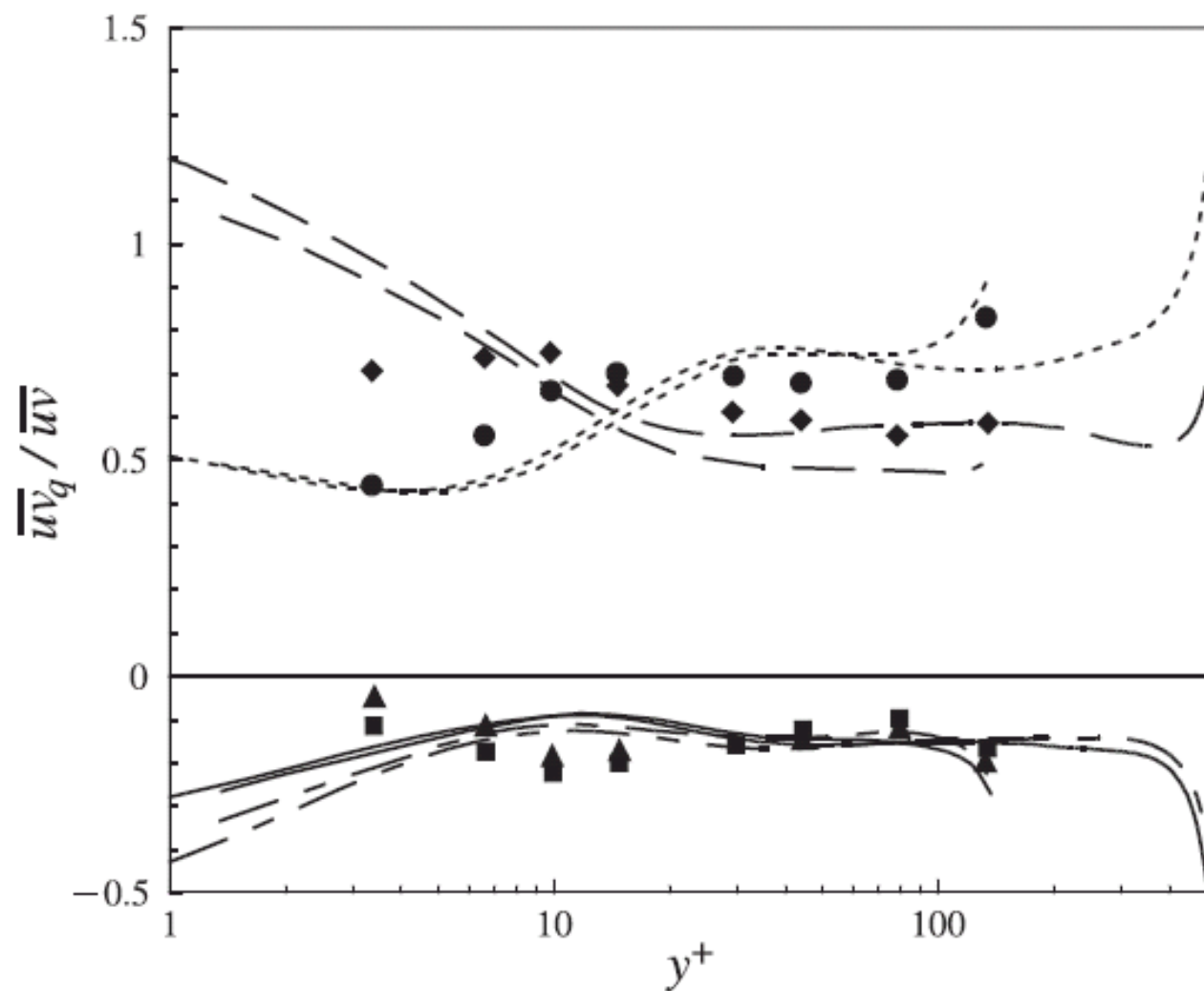


Fig. 4.31 Quadrant decomposition of Reynolds shear stress in a channel flow. DNS at $R_\tau = 180$ [37] and 590 [49] and experiment [66] at $R_\tau = 187$: ■ and ---, Q1; ● and ⋯, Q2; ▲ and —, Q3; ◆ and — —, Q4.

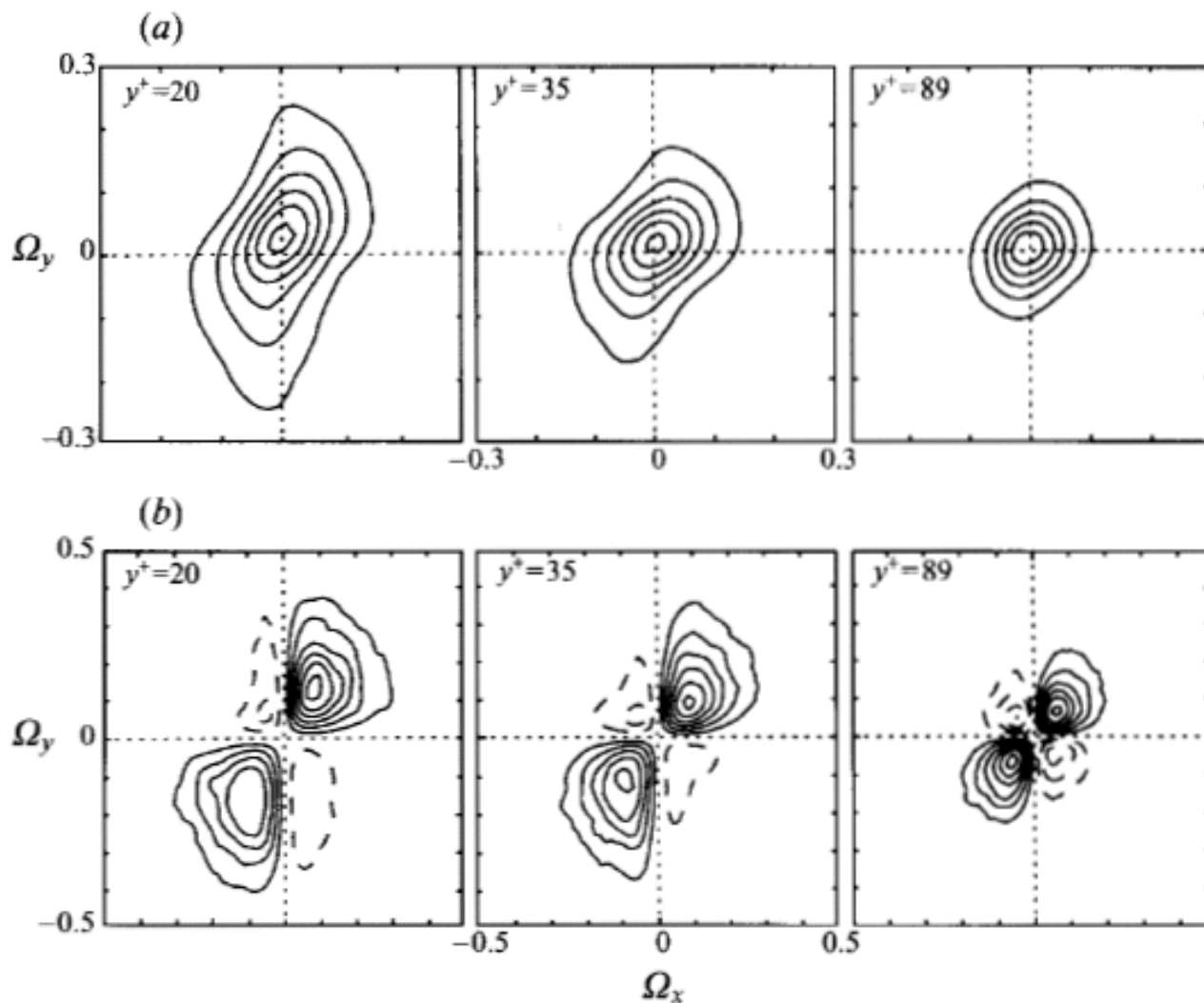


FIGURE 11. (a) JPDFs and (b) covariance integrands of Ω_x and Ω_y , non-dimensionalized by v/u_τ^2 . All vorticity and velocity gradients are normalized by this time scale here and in the following figures. Contour increments (for $y^+ = 20, 35$ and 89 , respectively) are (a) $3.3, 4.5, 9.0$ and (b) $3.4 \times 10^{-6}, 2.9 \times 10^{-6}, 1.4 \times 10^{-6}$. The outer contours are one increment above zero.

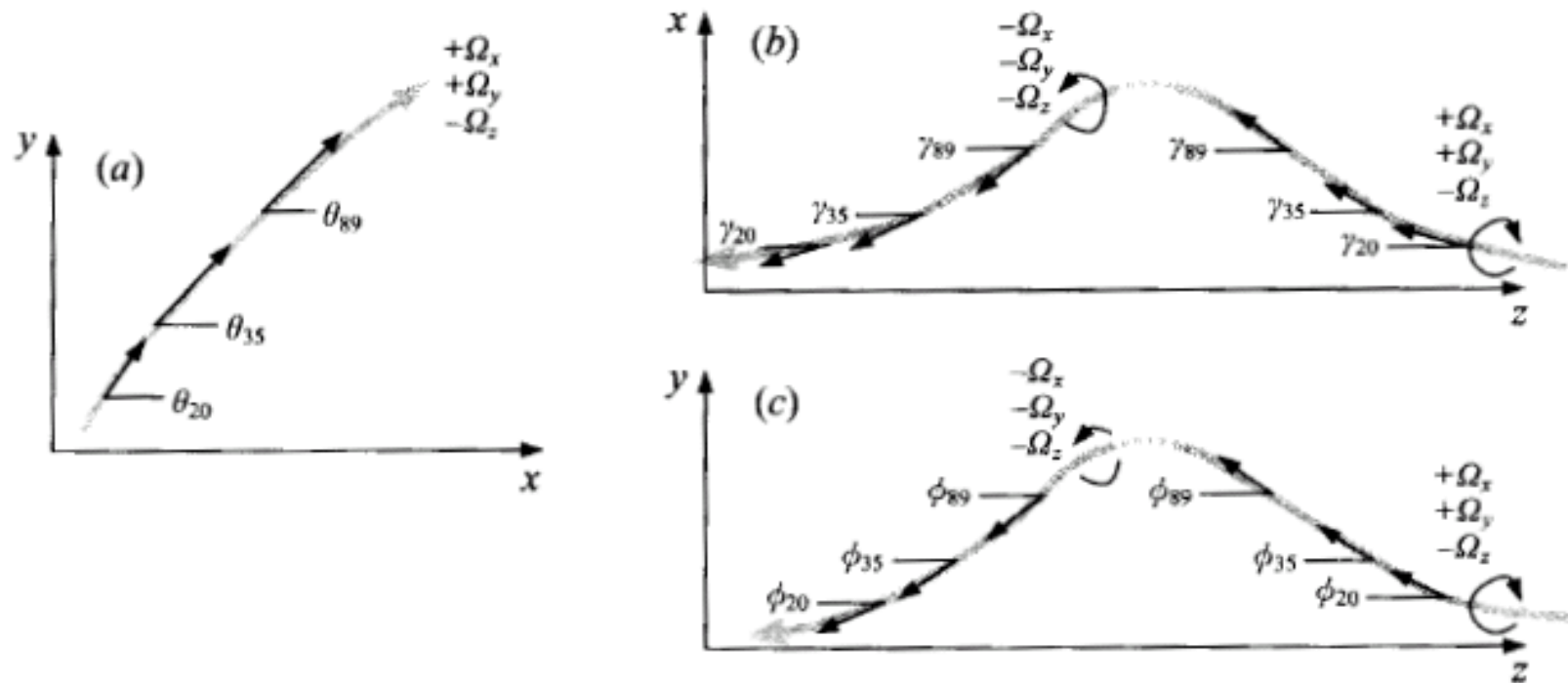
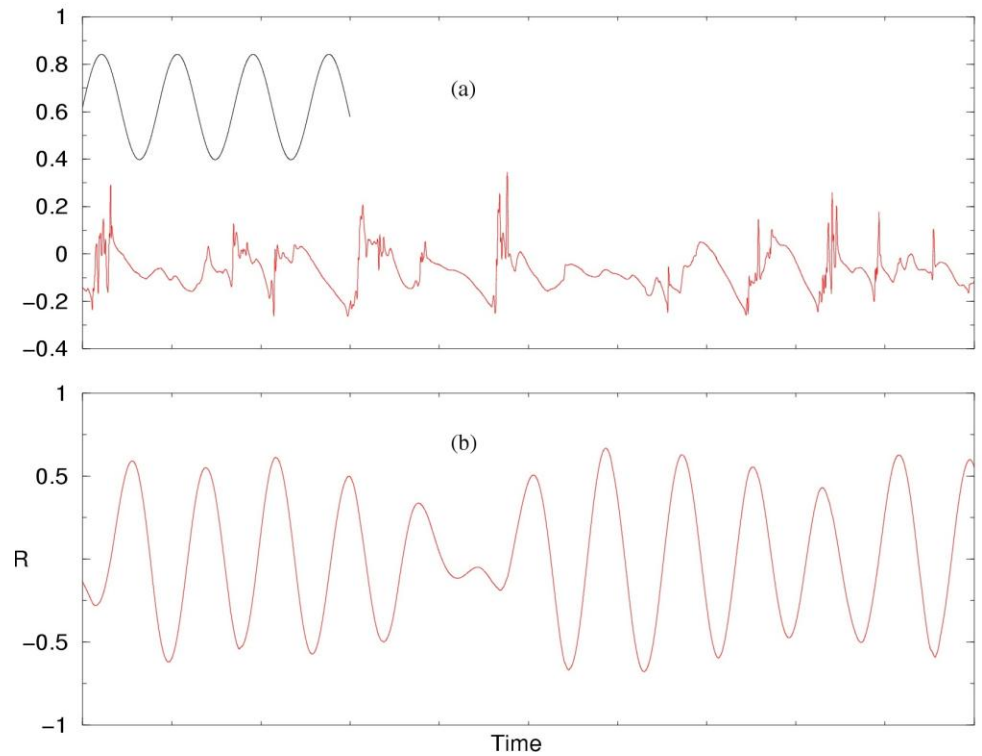
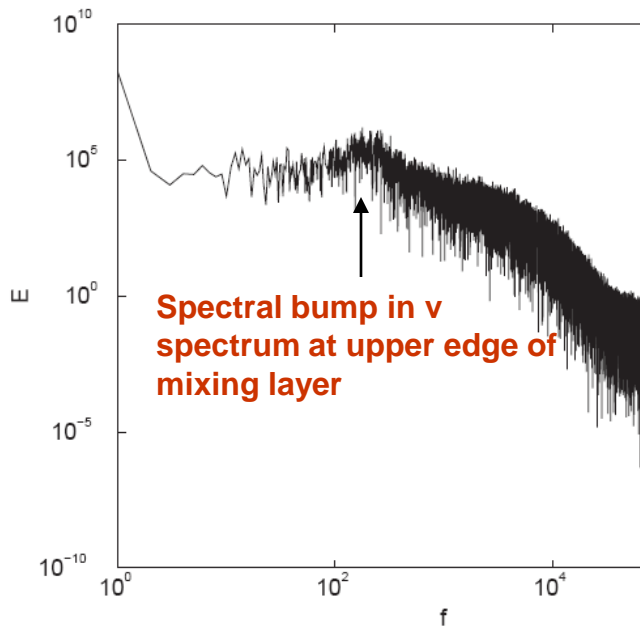
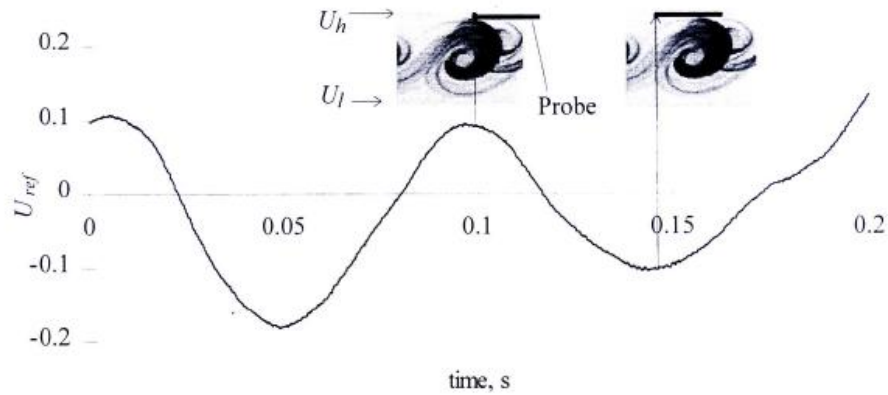
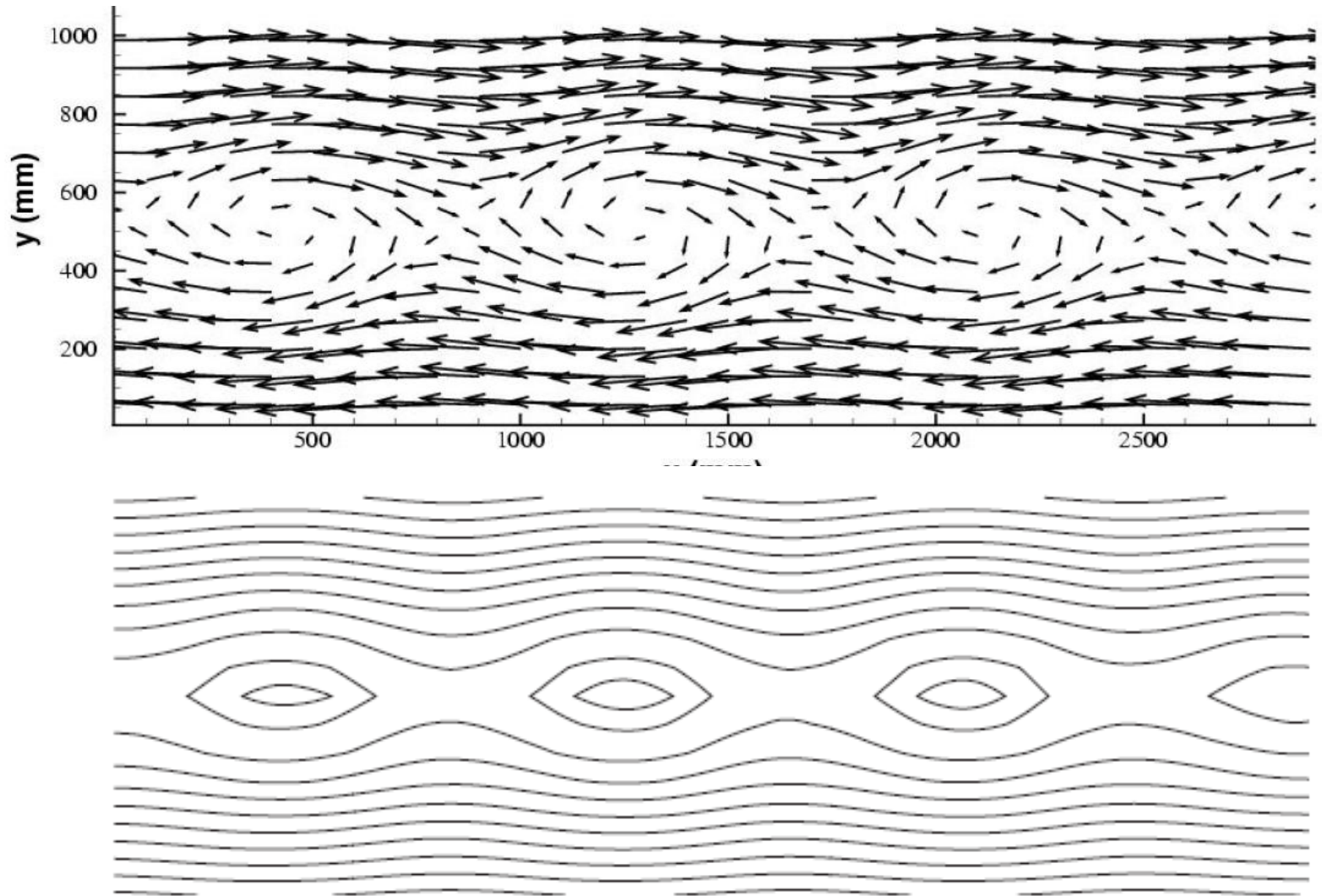


FIGURE 15. Projections of vorticity filament segments making the largest contributions to $\overline{\Omega_x \Omega_y}$, $\overline{\Omega_x \Omega_z}$ and $\overline{\Omega_y \Omega_z}$ at $y^+ = 20, 35$ and 89 . (a) Projection on (x, y) -plane where $\theta \equiv \tan^{-1}(\Omega_y/\Omega_x)$: $\theta_{20} \approx 58^\circ$ (or -118°) at $y^+ = 20$, $\theta_{35} \approx 48^\circ$ (or -136°) at $y^+ = 35$ and $\theta_{89} \approx 48^\circ$ (or -137°) at $y^+ = 89$. (b) Projection on (x, z) -plane where $\gamma \equiv \tan^{-1}(\Omega_x/\Omega_z)$: $\gamma_{20} \approx \pm 16^\circ$, $\gamma_{35} \approx \pm 27^\circ$ and $\gamma_{89} \approx \pm 42^\circ$. (c) Projection on (y, z) -plane where $\phi \equiv \tan^{-1}(\Omega_y/\Omega_z)$: $\phi_{20} \approx \pm 27^\circ$, $\phi_{35} \approx \pm 35^\circ$ and $\phi_{89} \approx \pm 37^\circ$.

Detection Method for Phase Averaging



Phase averaged velocity vectors in a moving frame of reference



$$\langle a(t) \rangle = \frac{1}{N} \sum_{n=1}^N a(\tau_n + t)$$

Phase Averaged Dissipation Rate & Vorticity Covariance

